Future Climates of South East Queensland: Results from High-Resolution Climate Modelling

Kim C. Nguyen and John L. McGregor

August 2012

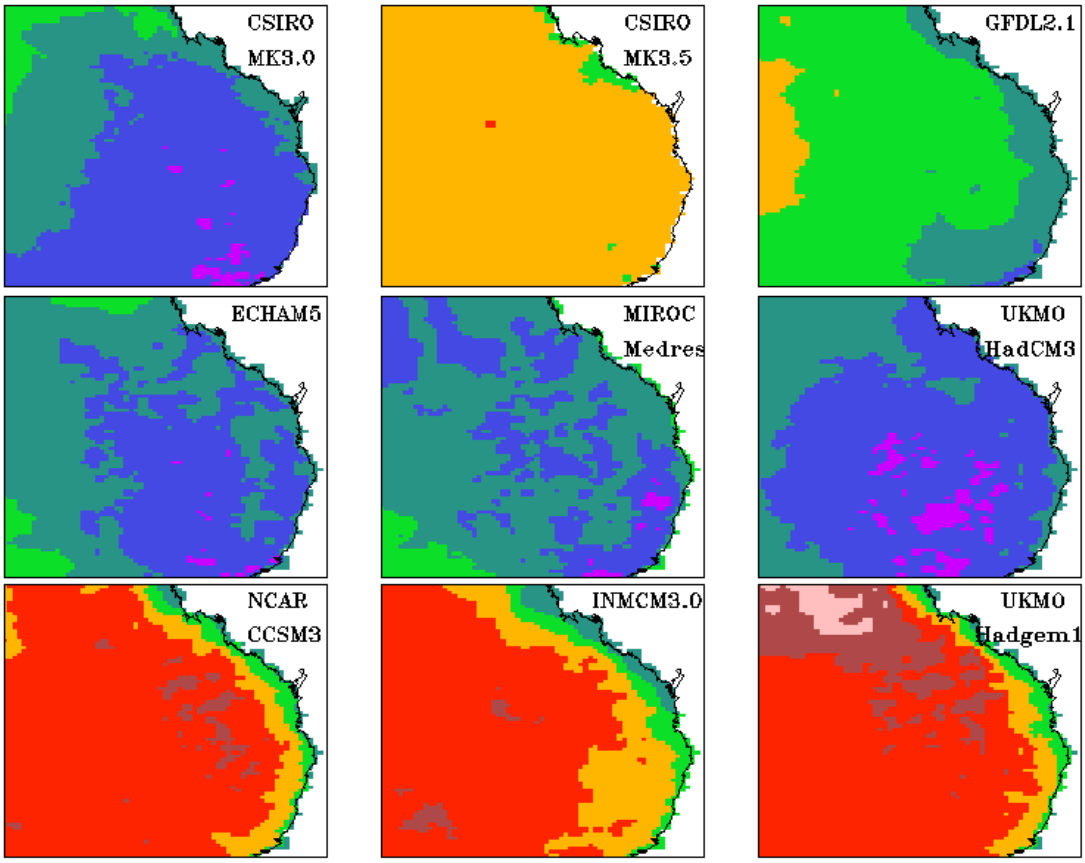

Urban Water Security Research Alliance
Technical Report No. 79

Queensland Government

National Research FLAGSHIPS Water for a Healthy Country CSIRO

Griffith UNIVERSITY

THE UNIVERSITY OF QUEENSLAND AUSTRALIA

Urban Water Security Research Alliance Technical Report ISSN 1836-5566 (Online)
Urban Water Security Research Alliance Technical Report ISSN 1836-5558 (Print)

The Urban Water Security Research Alliance (UWSRA) is a $50 million partnership over five years between the Queensland Government, CSIRO's Water for a Healthy Country Flagship, Griffith University and The University of Queensland. The Alliance has been formed to address South East Queensland's emerging urban water issues with a focus on water security and recycling. The program will bring new research capacity to South East Queensland tailored to tackling existing and anticipated future issues to inform the implementation of the Water Strategy.

For more information about the:

UWSRA - visit http://www.urbanwateralliance.org.au/
Queensland Government - visit http://www.qld.gov.au/
Water for a Healthy Country Flagship - visit www.csiro.au/org/HealthyCountry.html
The University of Queensland - visit http://www.uq.edu.au/
Griffith University - visit http://www.griffith.edu.au/

Enquiries should be addressed to:

The Urban Water Security Research Alliance
PO Box 15087
CITY EAST QLD 4002

Ph: 07-3247 3005
Email: Sharon.Wakem@qwc.qld.gov.au

Project Leader – Wenju Cai
CSIRO Marine and Atmospheric Research
ASPENDALE VIC 3195

Ph: 03-9239 4419
Email: Wenju.Cai@csiro.au

Authors: 1 – CSIRO

Nguyen., K.C. and McGregor, J.L. (2012). *Future Climates of South East Queensland: Results from High-Resolution Climate Modelling*. Urban Water Security Research Alliance Technical Report No. 79.

Copyright

© 2012 CSIRO. To the extent permitted by law, all rights are reserved and no part of this publication covered by copyright may be reproduced or copied in any form or by any means except with the written permission of CSIRO.

Disclaimer

The partners in the UWSRA advise that the information contained in this publication comprises general statements based on scientific research and does not warrant or represent the accuracy, currency and completeness of any information or material in this publication. The reader is advised and needs to be aware that such information may be incomplete or unable to be used in any specific situation. No action shall be made in reliance on that information without seeking prior expert professional, scientific and technical advice. To the extent permitted by law, UWSRA (including its Partner's employees and consultants) excludes all liability to any person for any consequences, including but not limited to all losses, damages, costs, expenses and any other compensation, arising directly or indirectly from using this publication (in part or in whole) and any information or material contained in it.

Cover Photograph:

Description: Change of maximum temperature (°C) for DJF for 2050 relative to 1985.
© CSIRO

ACKNOWLEDGEMENTS

This research was undertaken as part of the South East Queensland Urban Water Security Research Alliance, a scientific collaboration between the Queensland Government, CSIRO, The University of Queensland and Griffith University.

Particular thanks go to Christopher Bull for his help with proof reading of the report first draft and to Dr Marcus Thatcher and Dr Ramasamy Suppiah for his critical internal review.

FOREWORD

Water is fundamental to our quality of life, to economic growth and to the environment. With its booming economy and growing population, Australia's South East Queensland (SEQ) region faces increasing pressure on its water resources. These pressures are compounded by the impact of climate variability and accelerating climate change.

The Urban Water Security Research Alliance, through targeted, multidisciplinary research initiatives, has been formed to address the region's emerging urban water issues.

As the largest regionally focused urban water research program in Australia, the Alliance is focused on water security and recycling, but will align research where appropriate with other water research programs such as those of other SEQ water agencies, CSIRO's Water for a Healthy Country National Research Flagship, Water Quality Research Australia, eWater CRC and the Water Services Association of Australia (WSAA).

The Alliance is a partnership between the Queensland Government, CSIRO's Water for a Healthy Country National Research Flagship, The University of Queensland and Griffith University. It brings new research capacity to SEQ, tailored to tackling existing and anticipated future risks, assumptions and uncertainties facing water supply strategy. It is a $50 million partnership over five years.

Alliance research is examining fundamental issues necessary to deliver the region's water needs, including:

- ensuring the reliability and safety of recycled water systems.
- advising on infrastructure and technology for the recycling of wastewater and stormwater.
- building scientific knowledge into the management of health and safety risks in the water supply system.
- increasing community confidence in the future of water supply.

This report is part of a series summarising the output from the Urban Water Security Research Alliance. All reports and additional information about the Alliance can be found at http://www.urbanwateralliance.org.au/about.html.

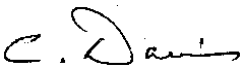

Chris Davis
Chair, Urban Water Security Research Alliance

CONTENTS

Acknowledgements i
Foreword ii
Executive Summary 1
1. Introduction 2
2. Results and Discussion 3
2.1. Rainfall 3
2.2. Maximum and Minimum Temperatures 12
2.3. Diurnal Temperature Range (DTR) 18
2.4. Solar Radiation 21
2.5. Relative Humidity 24
2.6. Wind Speed at 10 Metres 28
2.7. Pan Evaporation 31
3. Summary 34
References 35

LIST OF FIGURES

Figure 1: Change of DJF rainfall (mm/day), with the change for the 2050 period relative to 1985, where stippling indicates the change at the 95th significant level simulated by CCAM at 20 km resolution. 4
Figure 2: Rainfall change as in Figure 1 but for MAM 5
Figure 3: Rainfall change as in Figure 1 but for JJA. 5
Figure 4: Rainfall change as in Figure 1 but for SON. 6
Figure 5: Number of CCAM members that agree on rainfall change by 2050 relative to 1985, where +9 denotes that all nine members agree on increased rainfall, -9 denotes that all nine members agree on decreased rainfall. 7
Figure 6: Monthly rainfall change (upper panel, mm day-1) and percentage change (lower panels) at Toowoomba and Brisbane by 2050, relative to 1985. 7
Figure 7: Percentage change of rainfall rate for 2050 relative to 1985, from the CCAM 20 km simulations. 8
Figure 8: Percentage change of rainfall rate as in Figure 7 but for MAM. 9
Figure 9: Percentage change of rainfall rate as in Figure 7 but for JJA. 9
Figure 10: Percentage change of rainfall rate as in Figure 7 but for SON. 10
Figure 11: CCAM ensemble-mean seasonal rainfall change (mm per season) for 2050 relative to 1985. 11
Figure 12: CCAM ensemble-mean seasonal percent rainfall change for 2050 relative to 1985. 11
Figure 13: Change of maximum temperature (oC) for DJF for 2050 relative to 1985. 12
Figure 14: Change of maximum temperature as in Figure 13 but for MAM. 13
Figure 15: Change of maximum temperature as in Figure 13 but for JJA. 13
Figure 16: Change of maximum temperature as in Figure 13 but for SON. 14
Figure 17: Ensemble-mean change of the maximum temperature (oC) for 2050 relative to 1985. 14
Figure 18: Change of minimum temperature (oC) for DJF for 2050 relative to 1985. 15
Figure 19: Change of minimum temperature as in Figure 18 but for MAM. 16
Figure 20: Change of minimum temperature as in Figure 18 but for JJA. 16
Figure 21: Change of minimum temperature as in Figure 18 but for SON. 17
Figure 22: Ensemble-mean change of minimum temperature (oC) for 2050 relative to 1985. 17
Figure 23: Change (oC) in maximum and minimum temperature at Toowoomba and Brisbane by 2050 relative to 1985. 18
Figure 24: Change (ºC) in diurnal temperature range for DJF by 2050 relative to 1985. 19
Figure 25: As in Figure 24 but for MAM. 19
Figure 26: As in Figure 24 but for JJA. 20
Figure 27: As in Figure 24 but for SON. 20
Figure 28: Seasonal change of the CCAM ensemble-mean DTR (oC) by 2050 relative to 1985. 21
Figure 29: Change of solar radiation (W m-2) reaching the surface for DJF by 2050 relative to 1985. 22
Figure 30: Change of solar radiation as in Figure 29 but for MAM. 22
Figure 31: Change of solar radiation as in Figure 29 but for JJA. 23
Figure 32: Change of solar radiation as in Figure 29 but for SON. 23
Figure 33: Percent change of CCAM ensemble-mean solar radiation (W m-2) reaching the surface by 2050 relative to 1985. 24
Figure 34: Change of relative humidity (%) at 850 hPa for DJF by 2050 relative to 1985. 25
Figure 35: Change of relative humidity as in Figure 34 but for MAM. 25
Figure 36: Change of relative humidity as in Figure 34 but for JJA. 26
Figure 37: Change of relative humidity as in Figure 34 but for SON. 26
Figure 38: Change in relative humidity (%) at 850 hPa of the CCAM ensemble mean by 2050 relative to 1985. 27
Figure 39: Change in relative humidity as in Figure 38 but at upper levels (200 hPa). 27
Figure 40: Change in wind speed (km hour-1) at 10 m for DJF by 2050 relative to 1985. 28
Figure 41: Change in wind speed as in Figure 40 but for MAM. 29
Figure 42: Change in wind speed as in Figure 40 but for JJA. 29
Figure 43: Change in wind speed as in Figure 40 but for SON. 30
Figure 44: Change in wind speed as in Figure 40 but for percent change in CCAM ensemble mean. 30
Figure 45: Change in pan evaporation (W m-2) for DJF by 2050 relative to 1985. Significance is at 95th level over most of the region, but not separately shown for clarity. 31
Figure 46: Change in pan evaporation as in Figure 45 but for MAM. 32

Figure 47: Change in pan evaporation as in Figure 45 but for JJA. 32
Figure 48: Change in pan evaporation as in Figure 45 but for SON. 33
Figure 49: Percent change of ensemble-mean pan evaporation by 2050 relative to 1985. 33

LIST OF TABLES

Table 1: Future change of maximum and minimum temperatures (°C) and rainfall (mm day^{-1}) by 2050 relative to 1985. This change is averaged (land only) over the SEQ region (144°E-154°E, 33°S-21°S). Italics and underline numbers denote warmer and wetter; bold denote warmer and drier; other numbers denote warmer and no change in rainfall. 3

EXECUTIVE SUMMARY

The results presented in this report are based on simulations from the CSIRO Conformal Cubic Model (CCAM) at fine horizontal resolution of 20 kilometres (km) over South East Queensland (SEQ) and coarse resolution elsewhere. Climate change simulations were performed from 1971 to 2100 for the A2 emissions scenario. The study focuses on basic important variables associated with future planning of water resources over the region. These variables are rainfall, maximum and minimum temperatures, solar radiation reaching the surface, relative humidity, wind speed at 10 m and pan evaporation. The changes in selected variables are calculated as the mean differences between the period from 2036 to 2065 (centred on 2050) and from 1971 to 2000 (centred on 1985).

CCAM simulates increased rainfall in December to February (DJF); an increase by 10-15% for the future. However, CCAM simulates decreases in rainfall in March to May (MAM) and September to November (SON). Rainfall decline is stronger over the coastal regions compared to inland regions. The driest season is MAM, with rainfall reduction up to 15% around the coast. Moreover, the drier condition in MAM and SON has strong agreement between the CCAM ensemble members; all nine models in MAM and eight of the nine models in SON. For the wetter condition in DJF in the southern domain, only about half of the CCAM ensemble members agree on the rainfall increase. Future climates at two locations, representing inland (Toowoomba) and coastal (Brisbane) regions are also investigated. Except for DJF, there is a small decrease in rainfall at Toowoomba and Brisbane, with a reduction of around 1 mm/day or -10%. Rainfall reduction is greatest in September, by up to 20% at Toowoomba and by up to 15% at Brisbane.

CCAM simulates a warmer climate by 2050 from the baseline condition (1985). SON shows the greatest increase, up to 3°C in the maximum temperature and a slightly smaller increase in the minimum temperature for the inland region. The coast is predicted to have less warming compared to the inland region. By 2050, the maximum and minimum temperatures are projected to increase around 1.5-2.5^{o}C, with the temperatures at Toowoomba increasing more than those at Brisbane. The projected change in the diurnal temperature range (DTR) patterns reveals that, in DJF, the minimum temperature increases faster than the maximum temperature, but with less than half of the ensemble members agreeing on this change. In SON, the maximum temperature is projected to increase more than the minimum temperature for most of the region, in particular over the southern part of the domain where eight out of nine model ensemble members agree. In June to August (JJA), all nine model members agree in simulating that the minimum temperatures increase faster than the maximum temperatures along the coast; in MAM seven members agree on this faster increase.

The report summarises average changes over the SEQ region for maximum and minimum temperatures and for rainfall. The CCAM simulations show that the SEQ region as a whole will become warmer and drier (58% of the simulations), warmer and wetter (25% of the simulations) and warmer and no change in rainfall (17% of the simulations), by 2050 compared to 1985.

The CCAM simulations also show solar radiation increases over the northern part of the domain in DJF, along the north-east coast in MAM and in the southern part of the domain in JJA and almost everywhere in SON. However the percent increase is small - less than 3%. For relative humidity, consistent with the future warmer climate described above, the 850 hPa relative humidity is projected to increase in DJF and decrease in the other seasons. However, an opposite direction of change is projected for the relative humidity in the upper levels of the atmosphere (around 200 hPa), with a gradual increase from north to south. These results suggest that, in future, except for DJF, air near the surface will become warmer and drier, but more moist aloft.

For wind speeds at 10 m above the ground, in general the near-surface winds are projected to be weaker in DJF, with the largest reduction seen in the northern part of the domain and along the coast. However, wind speeds are projected to increase in SON and in other seasons, except for the coastal region.

A combined effect of the increase in solar radiation and the increased surface wind speeds leads to an increase in pan evaporation. The pan evaporation is simulated to increase everywhere, with the largest increases expected in SON. This result is consistent with the reduction in rainfall in SON as described above.

1. INTRODUCTION

Climate is a very complex natural system and its future changes are also likely to be complex. We cannot simply extrapolate past trends to provide future climate projections. Instead, it is necessary to use global numerical models which solve sets of mathematical equations that represent the Earth climate system.

In this study, simulations are performed for the current and future climates over the Australian continent from 1971 to 2100, downscaling from nine host GCMs: CSIRO Mk3.0, CSIRO Mk3.5, GFDL2.1, ECHAM5, MIROC-Medres, UKMO HadCM3, UKMO-Hadgem1, NCAR CCSM3 and INMCM3.0. These are coupled atmosphere-ocean GCMs, run for the A2 emissions scenario, as described in the Intergovernmental Panel on Climate Change (IPCC) Fourth Assessment Report (AR4) www.ipcc.ch/pdf/special-reports/spm/sres-en.pdf. The coupled GCMs in particular provide sea surface temperature (SST) and sea-ice for the CSIRO Conformal Cubic Model (CCAM) quasi-uniform 200 km grid global simulations, which are further downscaled to about 20 km resolution for the South East Queensland (SEQ) region. The downscaling process provides output for a comprehensive range of variables on a sub-daily time-scale at a resolution of around 20 km over much of eastern Australia. The meteorological variables for a region bounded by 33–21°S and 145–155°E are extracted from this dataset and analysed.

The main goal of this study is to use a high-spatial-resolution regional climate model (CCAM) to produce projections of future climate for SEQ. Details of the model description and set up are provided by Nguyen *et al*. (2011, 2012).

2. RESULTS AND DISCUSSION

This section discusses the climate changes for the time period 2036-2065 (centred on 2050) relative to 1971-2000 (centred on 1985) in the context of 30-year means. For each subsection, we first consider each CCAM member and then we consider the ensemble-mean (unweighted-mean over nine CCAM simulations). Variables such as rainfall, maximum and minimum temperatures, diurnal temperature range (DTR), solar radiation, 10 m wind speed (U10), low-level relative humidity and pan evaporation are used to investigate future change in the climate of the region. To account for uncertainty in the future climate, we report the future change for each CCAM simulation and the ensemble mean for all the above variables with significance level at the 95th level, using the Student test with different means. The stippling on the Figures shows the changes at the 95th significance level.

Averages changes over the SEQ region for maximum and minimum temperatures and for rainfall are summarised in Table 1.

Table 1: Future change of maximum and minimum temperatures (^{o}C) and rainfall (mm day^{-1}) by 2050 relative to 1985. This change is averaged (land only) over the SEQ region (144°E-154°E, 33°S-21°S). Italics and underline numbers denote warmer and wetter; bold denote warmer and drier; other numbers denote warmer and no change in rainfall.

	DJF			MAM			JJA			SON		
	Max	**Min**	**Rain**	**Max**	**Min**	**Rain**	**Max**	**Min**	**Rain**	**Max**	**Min**	**Rain**
CSIRO MK3.0	*1.0*	*1.2*	*0.4*	**1.4**	**1.4**	**-0.1**	1.2	1.4	0.0	*1.1*	*1.3*	*0.1*
CSIRO MK3.5	*2.3*	*2.4*	*0.2*	**2.5**	**2.4**	**-0.1**	2.2	2.2	0.0	**2.9**	**2.6**	**-0.2**
ECHAM5	*1.1*	*1.5*	*0.7*	**2.1**	**1.8**	**-0.3**	*1.8*	*2.1*	*0.1*	1.7	1.7	0.0
MIROC Medres	*1.1*	*2.0*	*0.9*	*1.8*	*2.3*	*0.3*	2.0	2.2	0.0	**2.5**	**2.6**	**-0.1**
GFDL_CM2.1	1.7	1.7	0.0	**2.4**	**2.2**	**-0.2**	**1.9**	**1.8**	**-0.1**	2.1	2.1	0.0
INMCM3_0	**2.7**	**2.0**	**-0.3**	**2.4**	**1.9**	**-0.3**	**2.1**	**1.5**	**-0.4**	**3.1**	**2.2**	**-0.5**
NCAR_CCSM3_0	**2.7**	**2.2**	**-0.4**	**2.2**	**2.1**	**-0.2**	**2.5**	**2.2**	**-0.2**	**3.0**	**2.6**	**-0.3**
UKMO Hadgem1	**2.8**	**2.0**	**-0.5**	*1.8*	*2.3*	*0.2*	**2.3**	**2.1**	**-0.3**	**3.2**	**2.3**	**-0.6**
UKMO HadCM3	*0.8*	*1.3*	*0.5*	**1.4**	**1.5**	**-0.1**	**1.6**	**1.7**	**-0.1**	**2.3**	**2.2**	**-0.1**

2.1. Rainfall

Figures 1 to 10 show CCAM-simulated rainfall changes (mm/season) and also percentage rainfall changes by 2050 for four seasons, December-January-February (DJF), March-April-May (MAM), June-July-August (JJA) and September-October-November (SON).

For DJF (Figure 1), five out of nine CCAM simulations, CSIRO MK3.0, CSIRO MK3.5, ECHAM5, MIROC Medres and UKMO HadCM3, project that rainfall will increase. The changes are largest (30-40%) and statistically significant mainly inland, except for the wettest downscaled model, MIROC-Medres, where rainfall increases significantly over the whole domain. The downscaled GFDL2.1 model projects wetter conditions in the south and drier in the north, but this change is not statistically significant. Three CCAM simulations, namely, NCAR CCSM3, INMCM3.0 and UKMO Hadgem1 simulate a decrease in rainfall over most parts of the domain. However, the decrease is only statistically significant along the coast in NCAR CCSM3 and the northern part of the domain in UKMO Hadgem1, and statistically significant only for a very small region in INMCM3.0.

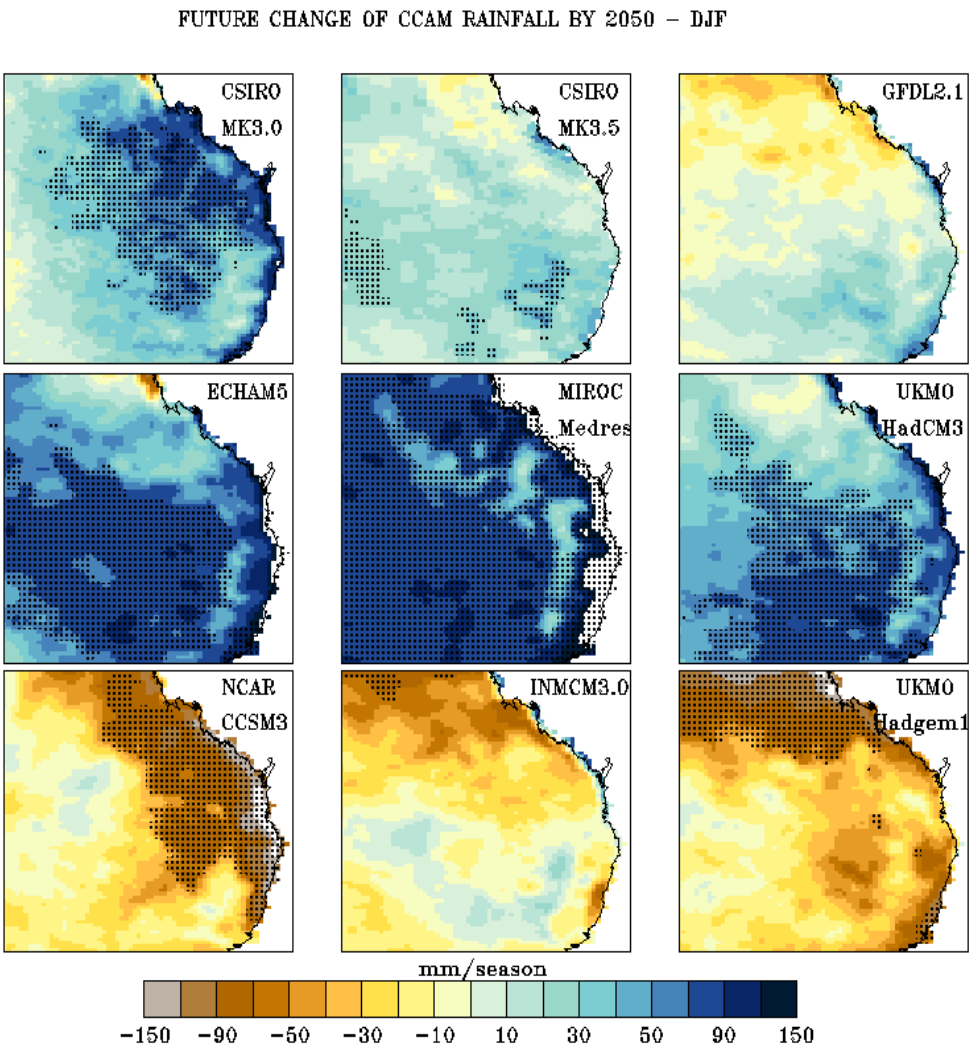

Figure 1: Change of DJF rainfall (mm/day), with the change for the 2050 period relative to 1985, where stippling indicates the change at the 95th significant level simulated by CCAM at 20 km resolution.

For MAM, most CCAM simulations project a decrease in rainfall (Figure 2), with the largest reduction along the coast and the northern part of the domain (ECHAM5). However, the region with statistically significant change is relatively small. CSIRO MK3.0, MIROC Medres, UKMO HadCM3 and UKMO Hadgem1 project a slight increase in rainfall for the inland region; however only MIROC Medres produces rainfall increases that are statistically significant.

Rainfall in general is predicted to decrease in JJA (Figure 3). The largest reduction is seen in INMCM3.0 and UKMO Hadgem1, with statistical significance at the 95% confidence level. NCAR CCSM3 and UKMO HadCM3 also predict rainfall decreases, with significant decreases in the southern part of the domain in NCAR CCSM3, but the decreases are not statistically significant in UKMO HadCM3. GFDL2.1 projects drier near the north coast, wetter inland and south; these changes do not lie within the 95% confidence level. CSIRO MK3.0 and ECHAM5 project wetter conditions in which none of the projected changes lie within the 95% confidence level.

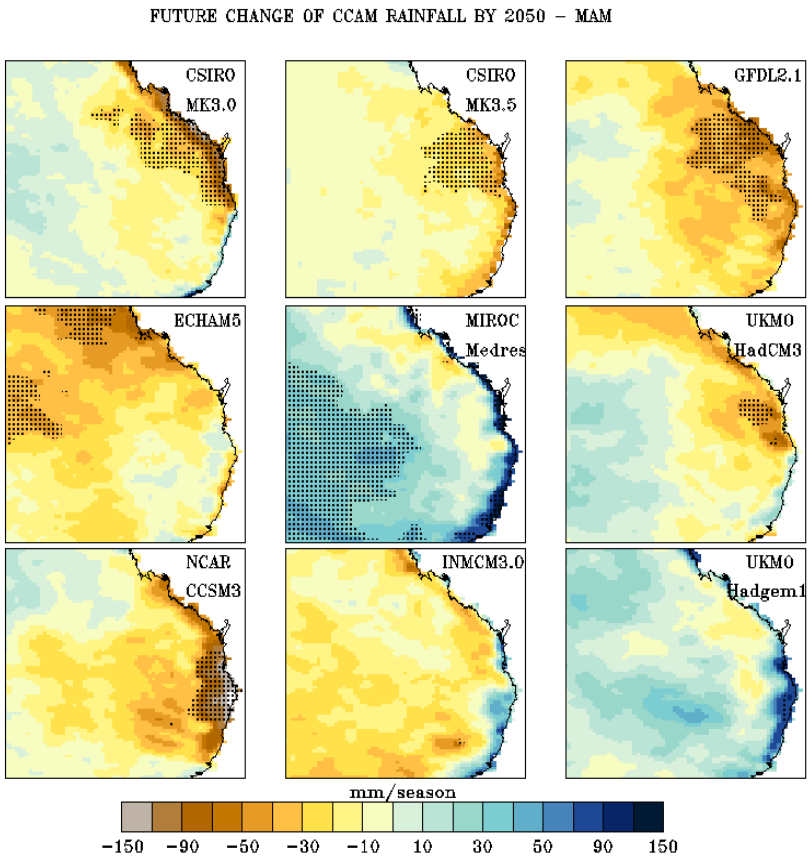

Figure 2: **Rainfall change as in Figure 1 but for MAM.**

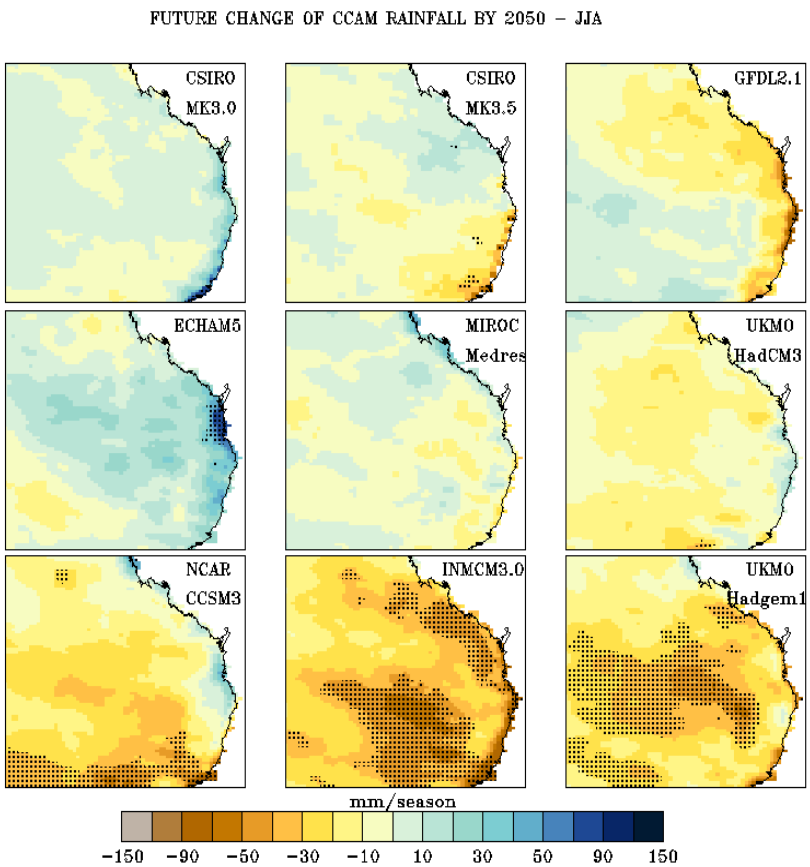

Figure 3: **Rainfall change as in Figure 1 but for JJA.**

Compared to other seasons, there is greater agreement between the CCAM simulations for SON (Figure 4). Rainfall decreases along the coast, with high significance seen in CSIRO MK3.5, INMCM3.0 and UKMO Hadgem1. The CSIRO_MK3.0 simulation seems to be an outlier, whereas GFDL2.1 and ECHAM5 have similar patterns of change.

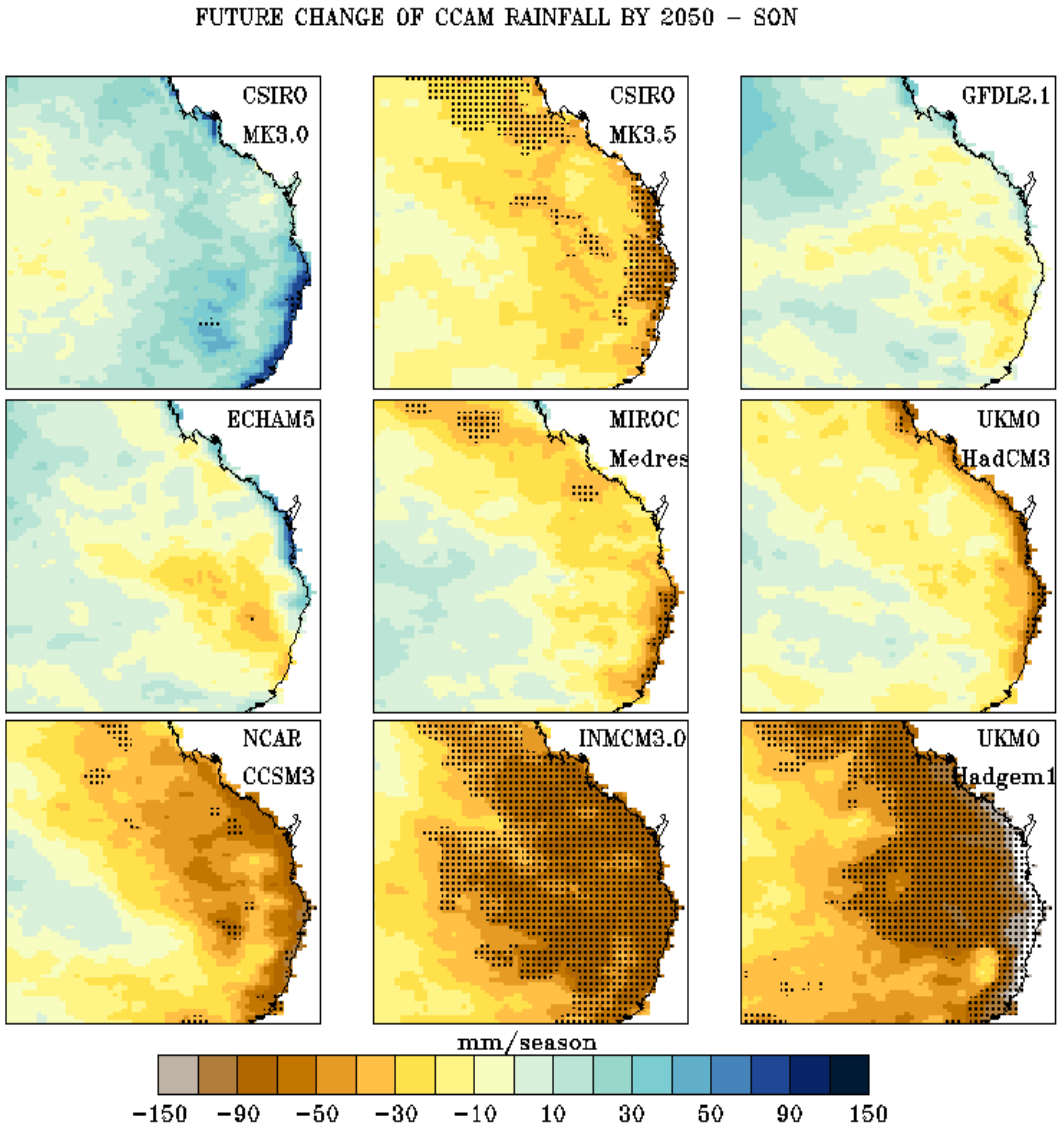

Figure 4: Rainfall change as in Figure 1 but for SON.

Figure 5 shows the number of CCAM ensemble members that agree on the rainfall changes for the four seasons. It is clear from Figure 2 that decreases in rainfall in MAM and SON have strong agreement among the CCAM ensemble members, with nine out of nine in MAM and eight out of nine in SON. The increase in rainfall in DJF in the southern part of the domain has only about half of the CCAM ensemble members in agreement.

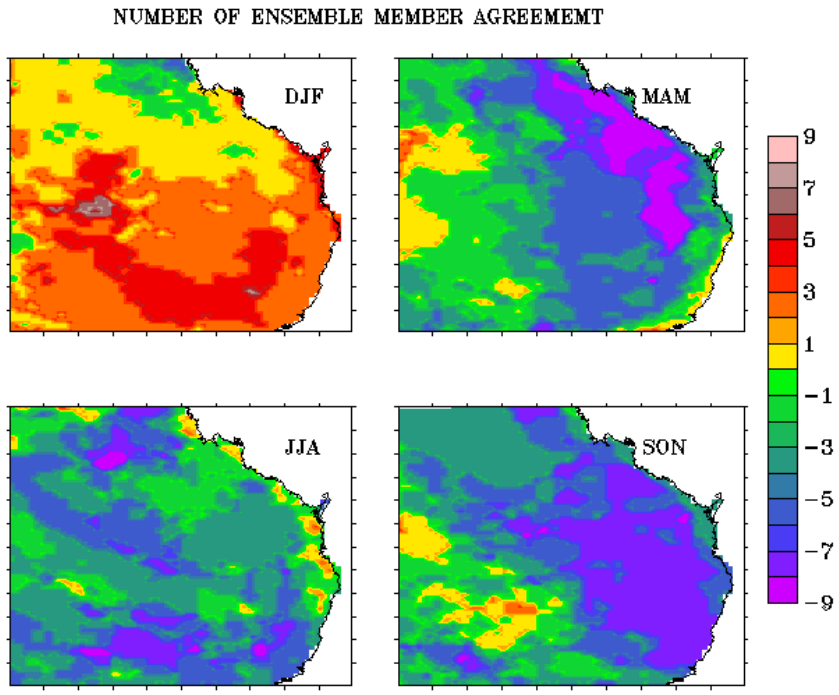

Figure 5: Number of CCAM members that agree on rainfall change by 2050 relative to 1985, where +9 denotes that all nine members agree on increased rainfall, -9 denotes that all nine members agree on decreased rainfall.

The CCAM simulations project decreases in rainfall for Toowoomba and Brisbane by 2050 with the largest reductions in September, up to 20% at Toowoomba and 15% at Brisbane (Figure 6). For other months, except December-January-February, the reduction is less than 1 mm/day, which translates into a percentage reduction of less than 10%.

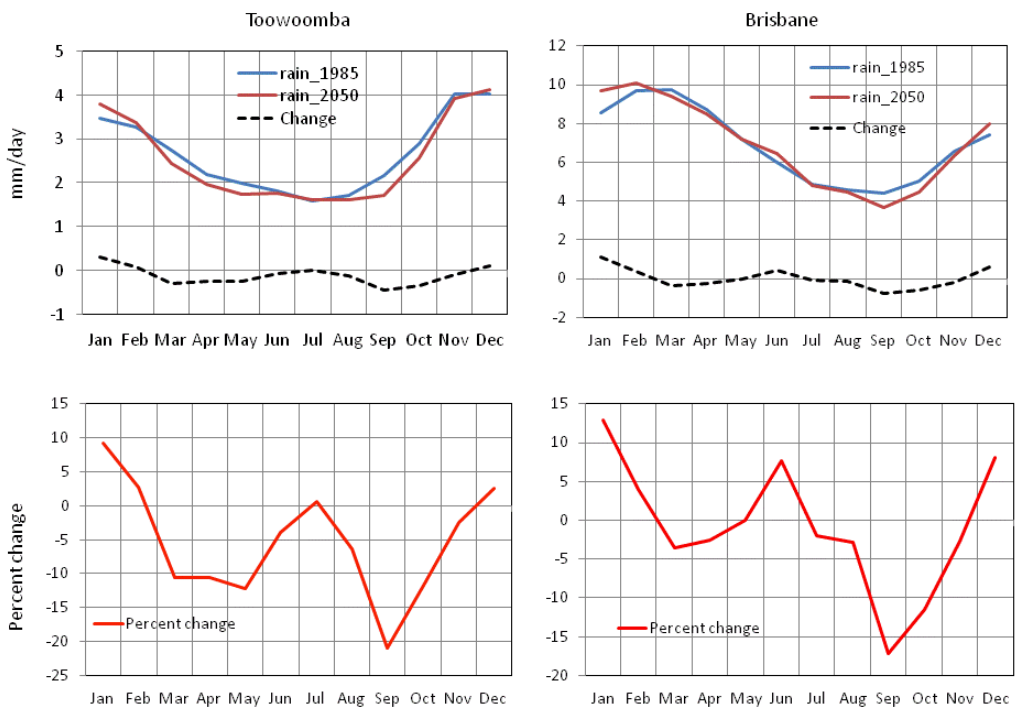

Figure 6: Monthly rainfall change (upper panel, mm day-1) and percentage change (lower panels) at Toowoomba and Brisbane by 2050, relative to 1985.

Percentage changes in rainfall for the four seasons are shown in Figures 7 to 10. For DJF (Figure 7), for the wetter conditions, the CCAM MIROC Medres simulation simulates the largest change, above +40% for the southwest corner of the domain, followed by ECHAM5 with around +30% change, then CSIRO MK3.0 and UKMO HadCM3 with rainfall increasing by 10-20%.

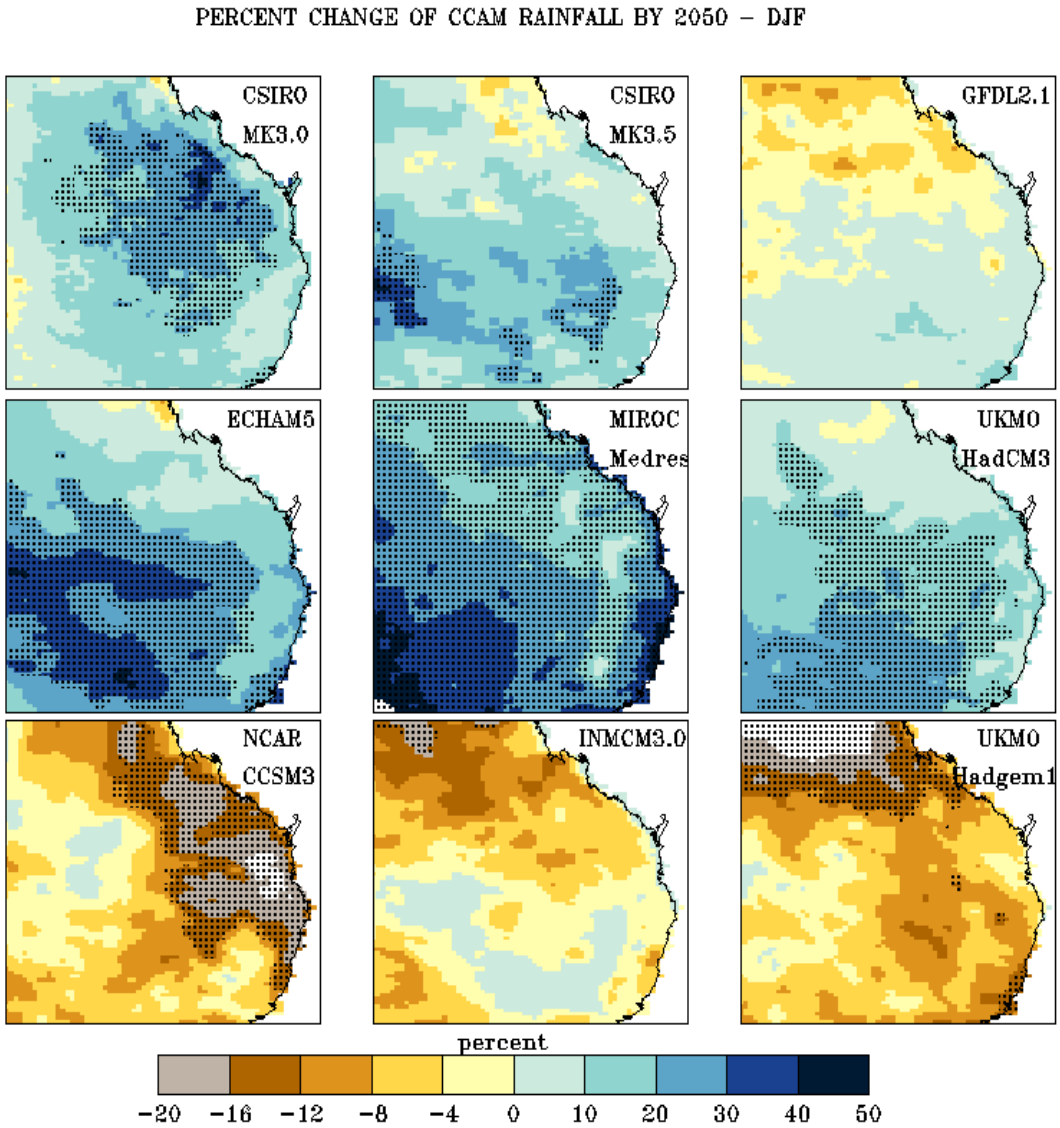

Figure 7: Percentage change of rainfall rate for 2050 relative to 1985, from the CCAM 20 km simulations.

For drier conditions, the largest percentage change is around -20% for the northern part of the domain in UKMO Hadgem1, and along the coast in NCAR CCSM3. For other seasons, the drier condition exceeds a 20% decline, such as from CSIRO MK3.5 and ECHAM5 in MAM (Figure 8), NCAR CCSM3, INMCM3.0 and UKMO Hadgem1 in JJA (Figure 9) and CSIRO MK3.5, INMCM3.0 and UKMO Hadgem1 in SON (Figure 10).

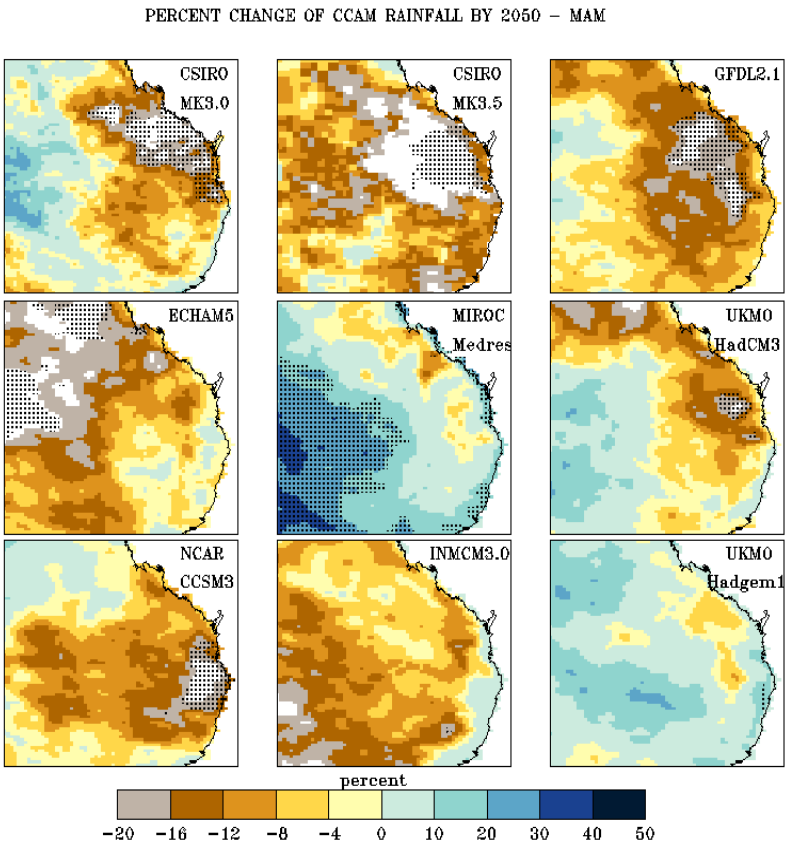

Figure 8: **Percentage change of rainfall rate as in Figure 7 but for MAM.**

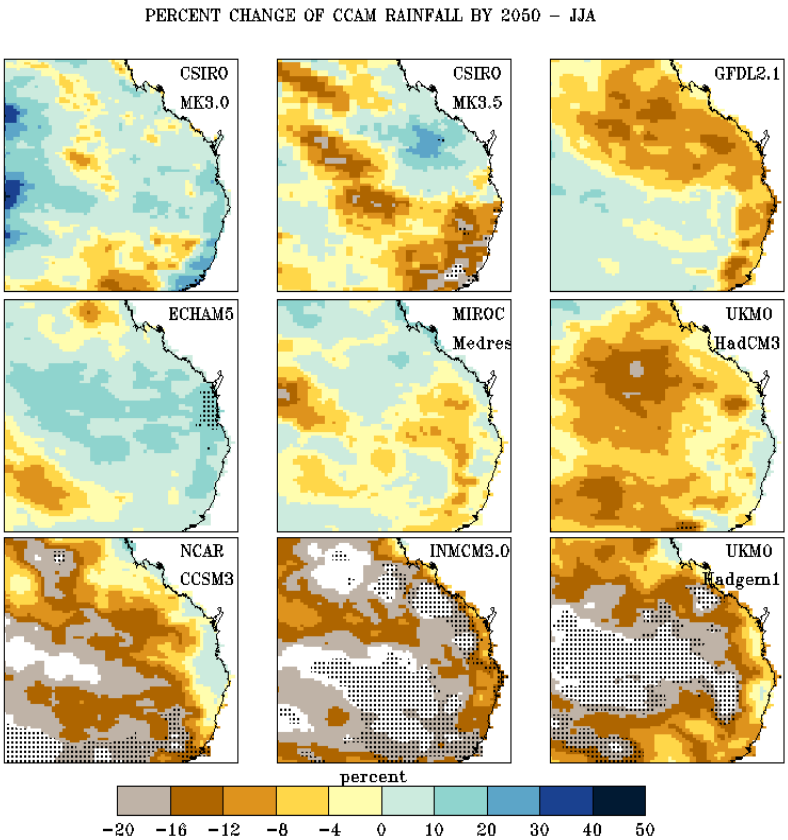

Figure 9: **Percentage change of rainfall rate as in Figure 7 but for JJA.**

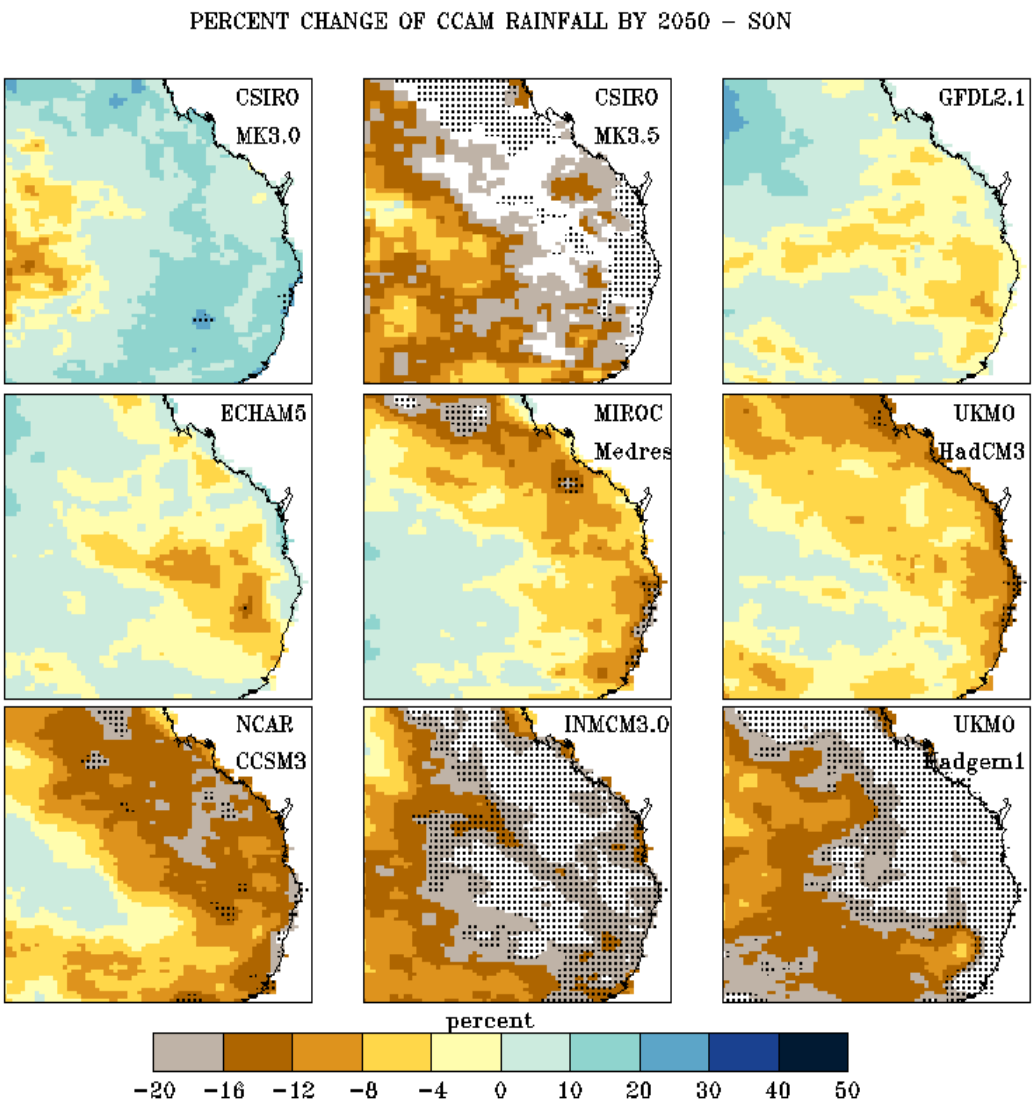

Figure 10: Percentage change of rainfall rate as in Figure 7 but for SON.

The ensemble-mean change in rainfall in mm per season (Figure 11) shows increases over most of the domain in DJF, being much wetter along the coast and south with percentage increases of around 15% (Figure 12, upper left panel), with smaller increases as one proceeds northwards. Rainfall is seen to decline along the coast in MAM (maximum decrease of around 15%) and SON. In JJA, the ensemble-mean projects drier conditions by 2050.

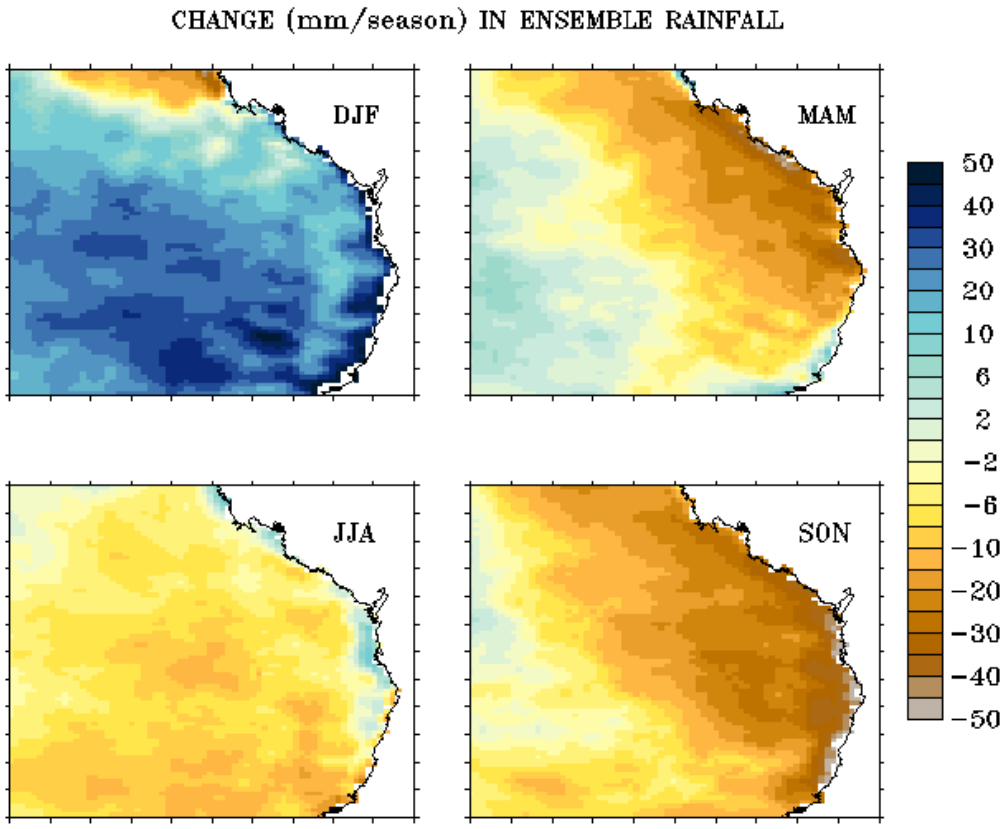

Figure 11: CCAM ensemble-mean seasonal rainfall change (mm per season) for 2050 relative to 1985.

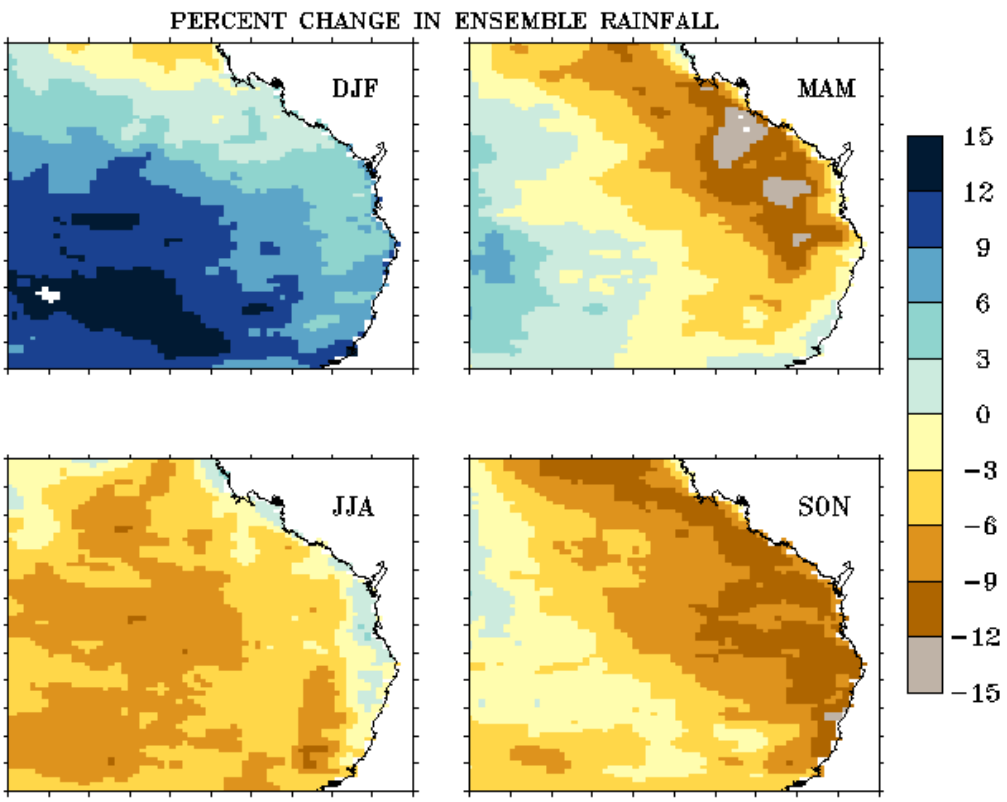

Figure 12: CCAM ensemble-mean seasonal percent rainfall change for 2050 relative to 1985.

2.2. Maximum and Minimum Temperatures

Future changes of the seasonal mean for maximum temperature for each CCAM simulation are shown in Figures 13 to 16, with their ensemble-mean changes shown in Figure 17. Simulated maximum temperature changes from the models are shown in Figures 13 to 16, and these changes can be summarised as follows:

- in DJF, increases of 1-2°C by CSIRO_MK3.0, ECHAM5, MIROC Medres and UKMO HadCM3; increases of 2-4°C by CSIRO MK3.5, NCAR CCSM3, INMCM3.0 and UKMO Hadgem1
- in MAM, increases of 1-2°C by CSIRO_MK3.0, UKMO HadCM3 and UKMO Hadgem1; increases of 2-3°C by CSIRO MK3.5, GFDL2.1, ECHAM5, MIROC Medres, NCAR CCSM3 and INMCM3.0
- in JJA, increases of 1-2°C by CSIRO_MK3.0 and UKMO HadCM3; increases of 2-3°C by the others
- in SON, increases of 1-2°C by CSIRO_MK3.0 and ECHAM5, increases of 2-4°C by the others; the largest warming is by UKMO Hadgem1.

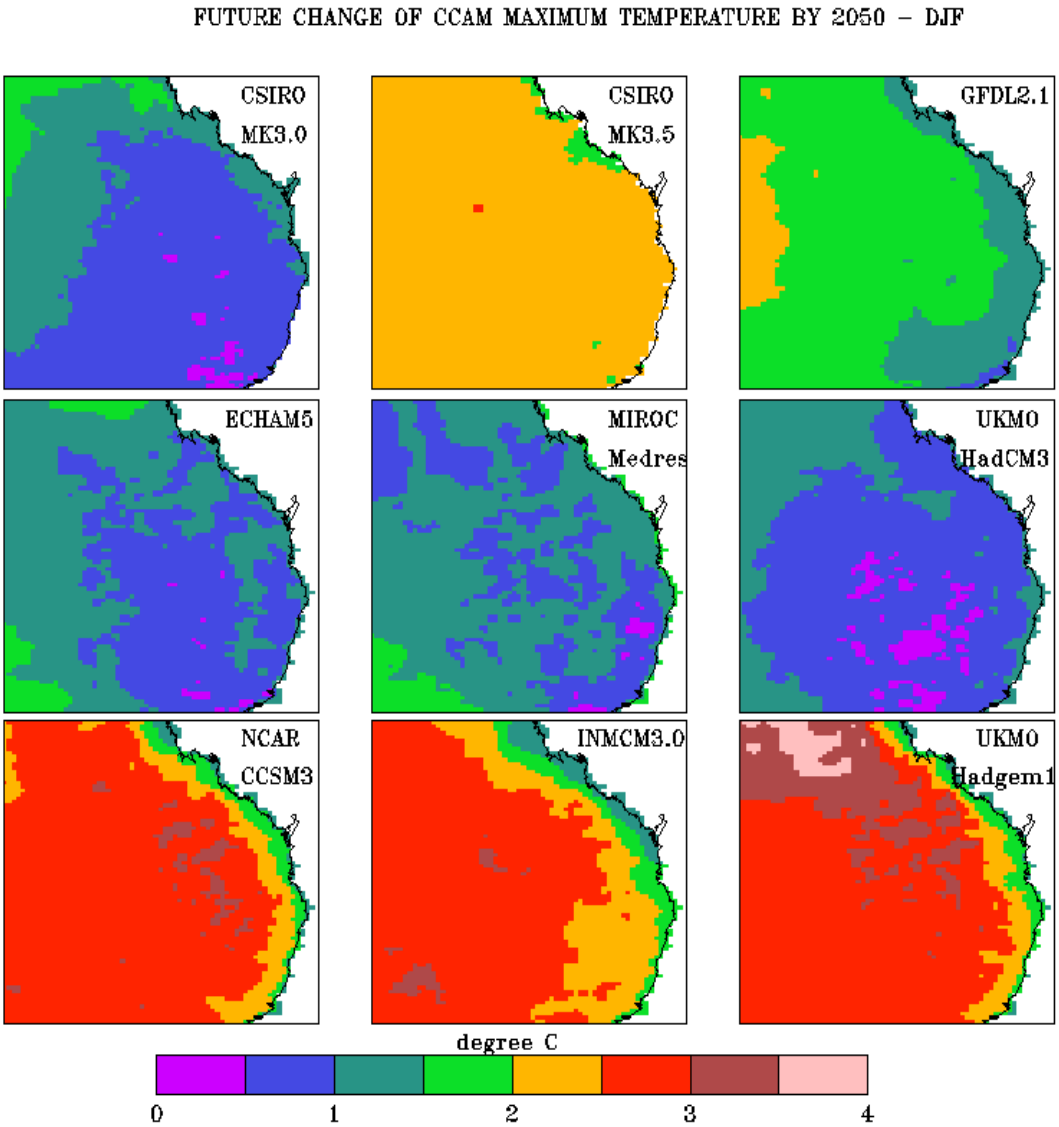

Figure 13: Change of maximum temperature (oC) for DJF for 2050 relative to 1985.

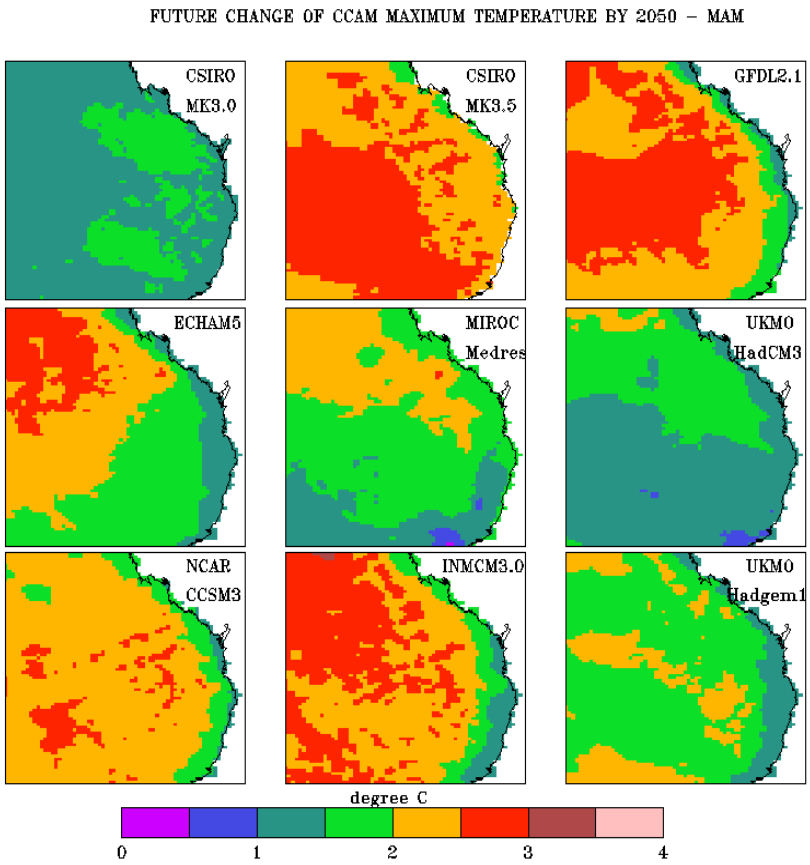

Figure 14: Change of maximum temperature as in Figure 13 but for MAM.

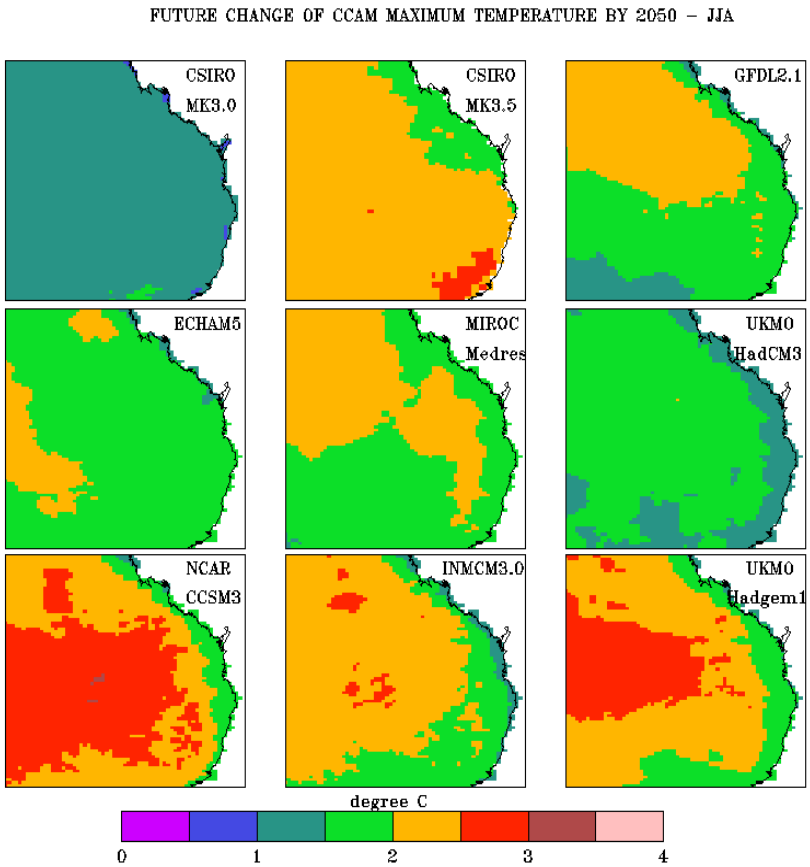

Figure 15: Change of maximum temperature as in Figure 13 but for JJA.

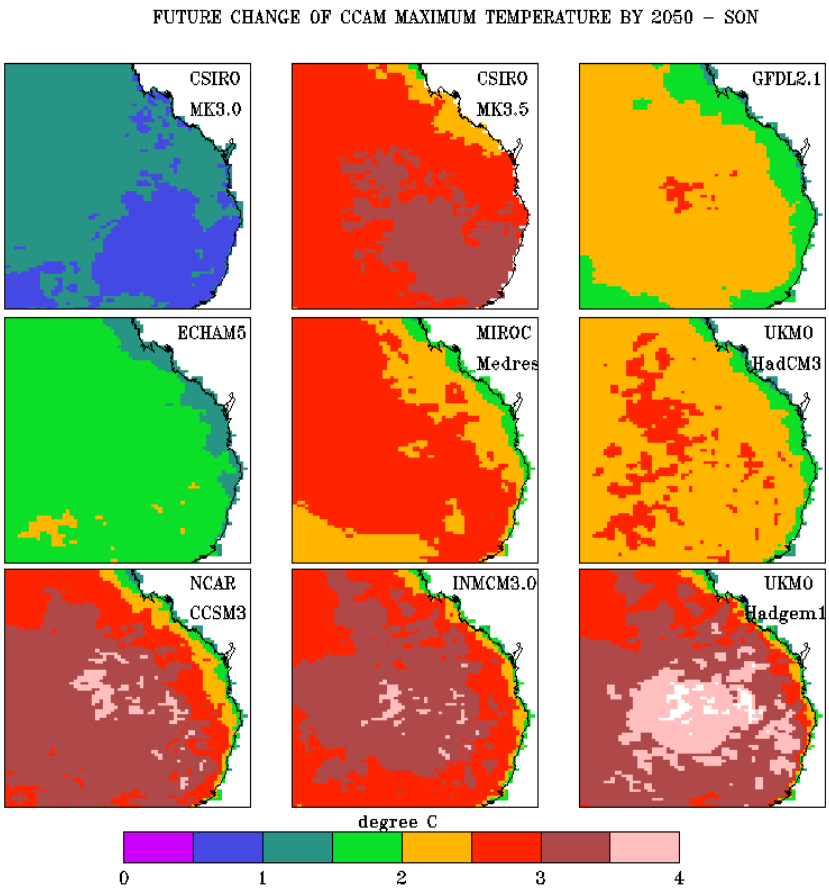

Figure 16: Change of maximum temperature as in Figure 13 but for SON.

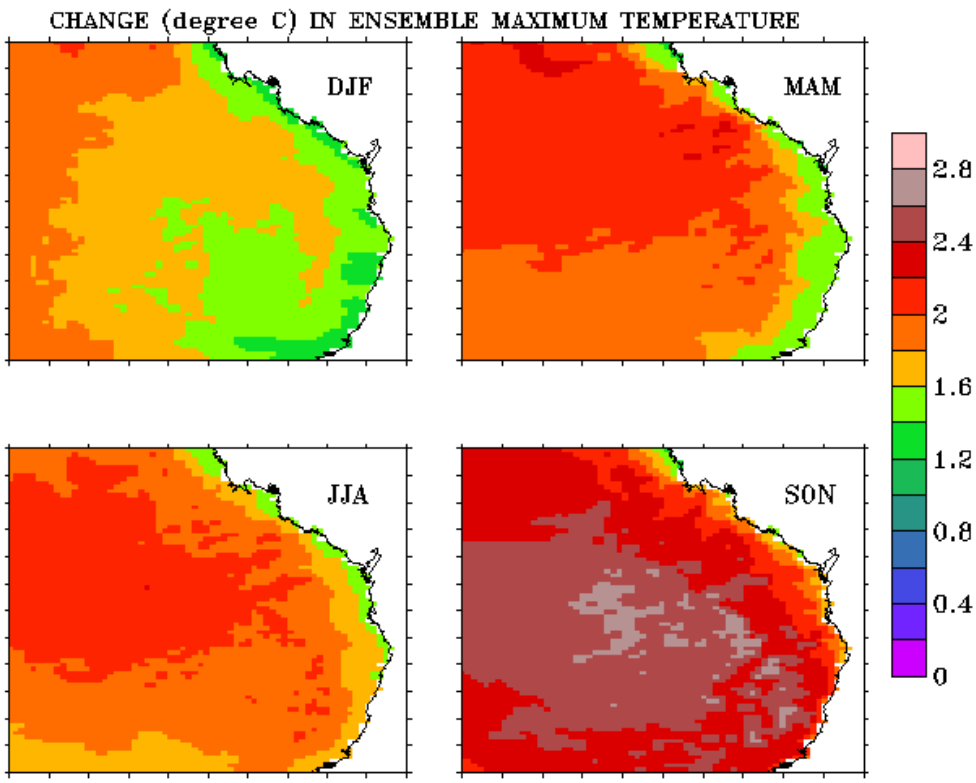

Figure 17: Ensemble-mean change of the maximum temperature (oC) for 2050 relative to 1985.

Future changes of minimum temperatures are shown in Figures 18 to 22. Simulated minimum temperature changes from the models are shown in Figures 18 to 21 and these changes can be summarised as follows:

- in DJF, increases of 1-2°C by CSIRO_MK3.0, ECHAM5, GFDL2.1 and UKMO HadCM3; increases of 2-3°C by CSIRO MK3.5, MIROC Medres, NCAR CCSM3, INMCM3.0 and UKMO Hadgem1
- in MAM, increases of 1-2°C by CSIRO_MK3.0 and UKMO HadCM3; increases of 2-3°C by CSIRO MK3.5, GFDL2.1, MIROC Medres, NCAR CCSM3, INMCM3.0 and UKMO Hadgem1
- in JJA, increases of 1-2°C by CSIRO_MK3.0, INMCM3.0 and UKMO HadCM3; increases of 2-3°C by CSIRO MK3.5, GFDL2.1, ECHAM5, MIROC Medres, NCAR CCSM3, and UKMO Hadgem1
- in SON, increases of 1-2°C for CSIRO_MK3.0 and ECHAM5; increases of 2-3.5°C for CSIRO MK3.5, GFDL2.1, MIROC Medres, NCAR CCSM3, INMCM3.0 and UKMO Hadgem1.

Simulated changes in maximum and minimum temperatures are statistically significant at the 95% confidence level, except for the maximum temperature in DJF from CSIRO_MK3.0, UKMO HadCM3, ECHAM5 and MIROC Medres, where the change is less than 1°C. The largest change is simulated in SON for both maximum and minimum temperatures.

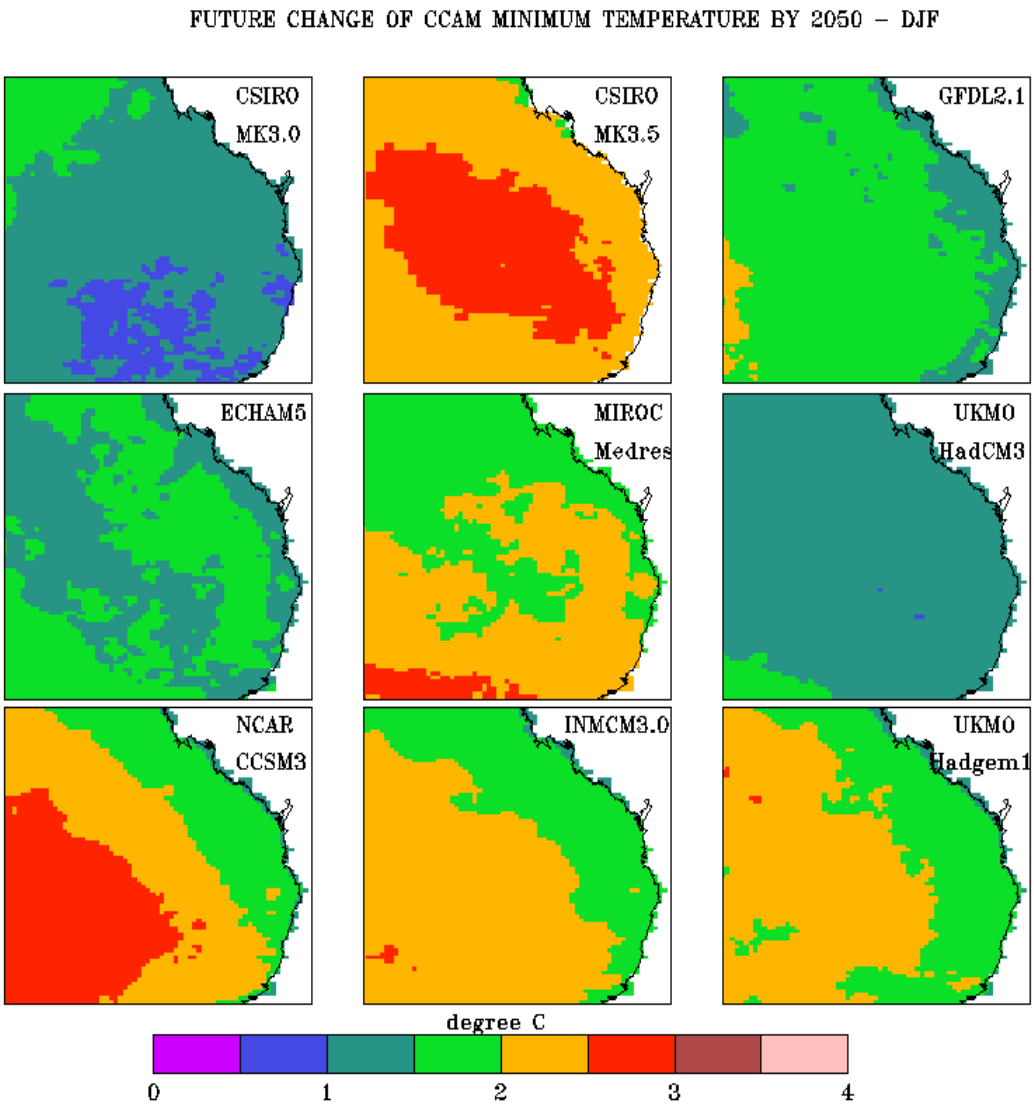

Figure 18: Change of minimum temperature (oC) for DJF for 2050 relative to 1985.

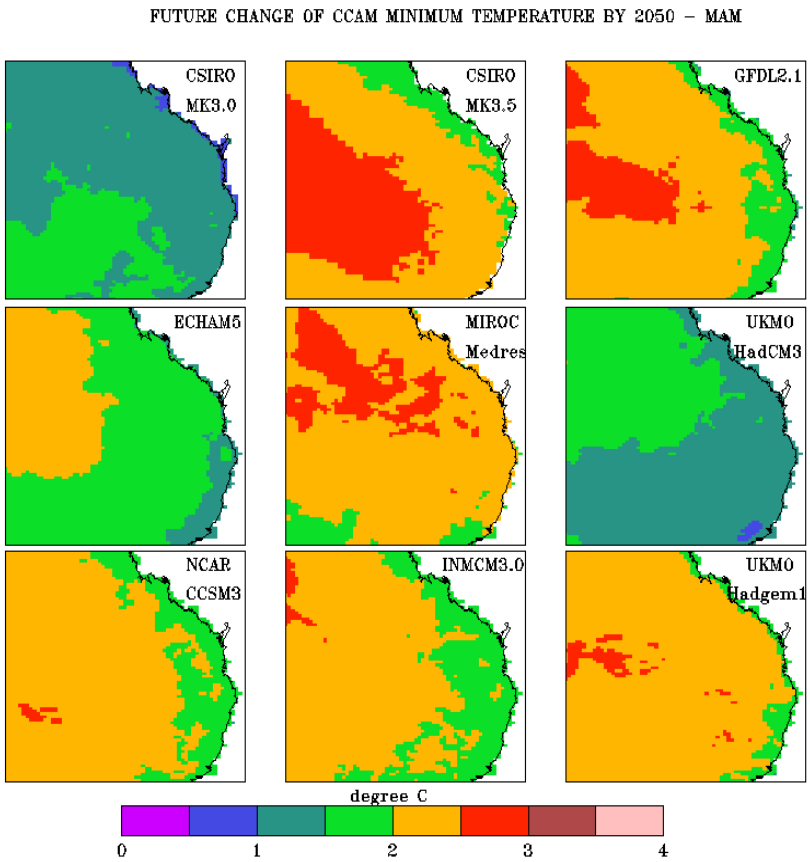

Figure 19: Change of minimum temperature as in Figure 18 but for MAM.

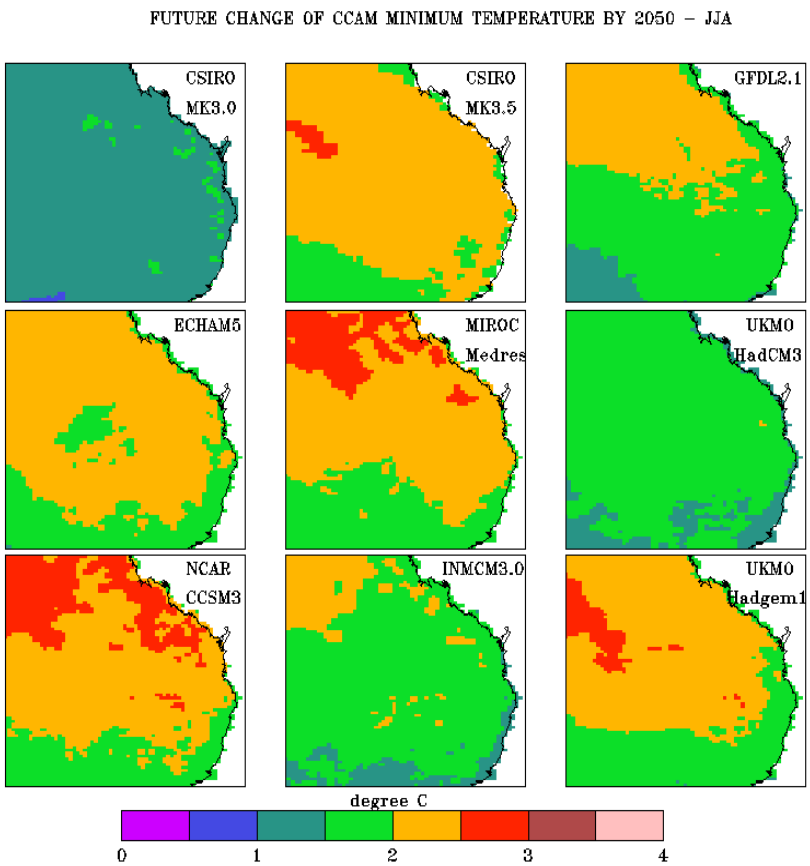

Figure 20: Change of minimum temperature as in Figure 18 but for JJA.

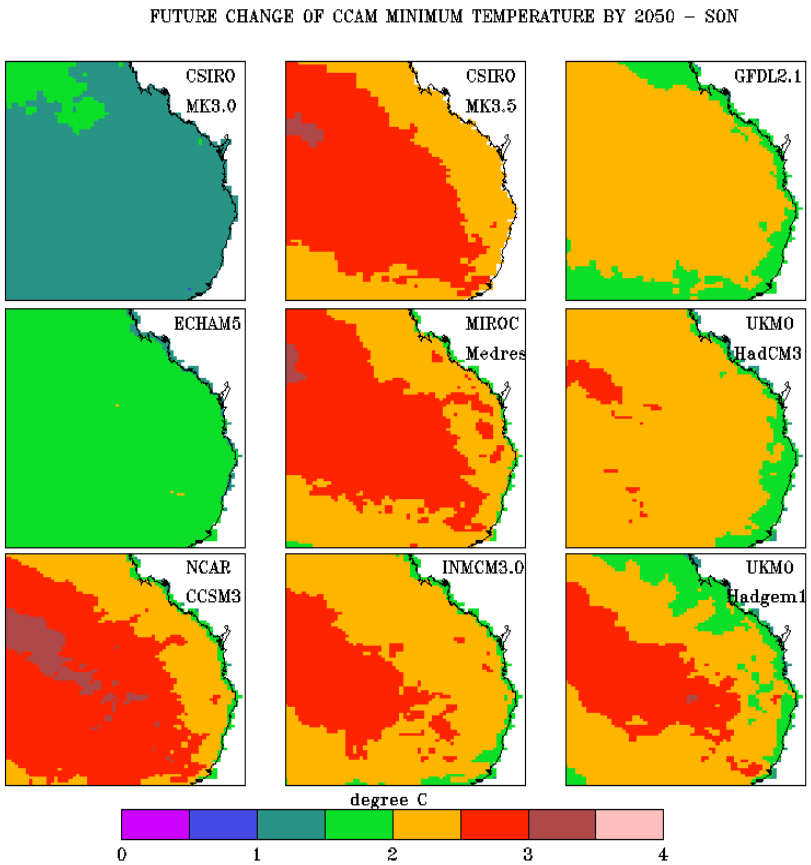

Figure 21: Change of minimum temperature as in Figure 18 but for SON.

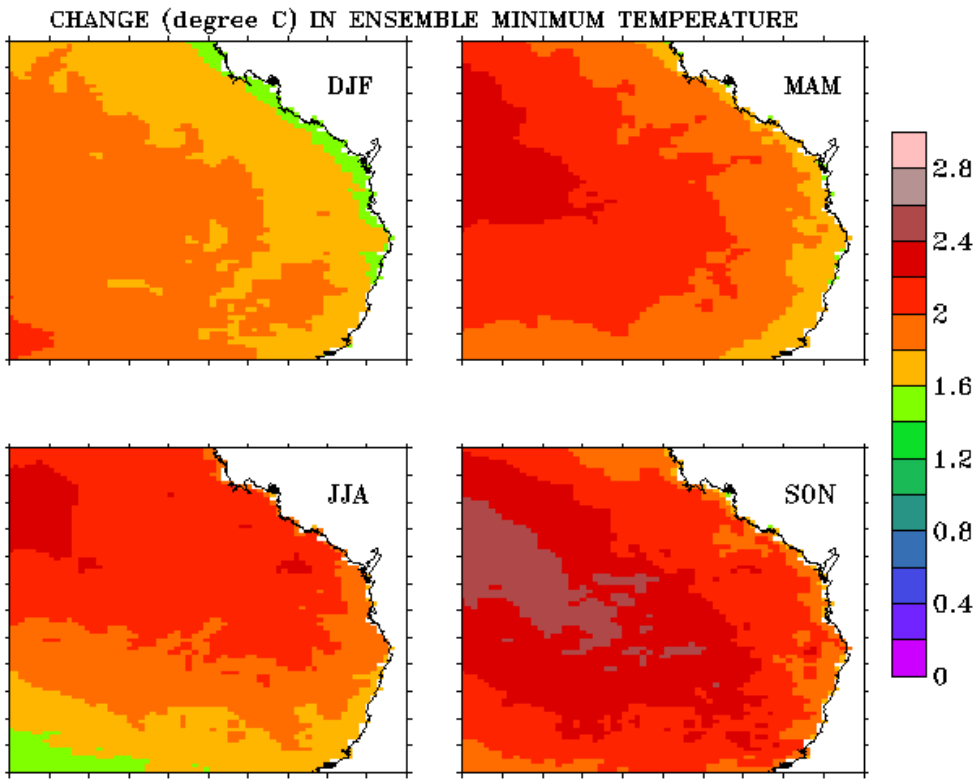

Figure 22: Ensemble-mean change of minimum temperature (oC) for 2050 relative to 1985.

The ensemble-mean maximum temperatures (Figure 17) and minimum temperatures (Figure 22) show similar increases of around 1-3°C, with largest increases in SON. All CCAM ensemble members strongly agree that both maximum and minimum temperatures will increase (not shown). A summary of each CCAM simulation of rainfall and maximum and minimum temperature changes by 2050 averaged over the SEQ region is shown in Table 1, where the italics and underline numbers denote warmer and wetter; bold denote warmer and drier; and other numbers denote warmer and no change in rainfall. There are thirty-six seasonal scenarios in total (nine CCAM simulations and four seasons). Results from Table 1 indicate warmer and wetter conditions for 25% of the total number of the simulated seasons, with increases for both rainfall and maximum/minimum temperatures. The warmer and drier condition, where maximum/minimum temperatures increase but rainfall decreases, is projected by 58% of the total number. Warmer conditions with no change in rainfall are simulated by 17% of the total number.

By 2050, maximum and minimum temperatures (Figure 23) are projected to increase by 1.5-2.5°C, with temperatures at Toowoomba set to increase more than those at Brisbane.

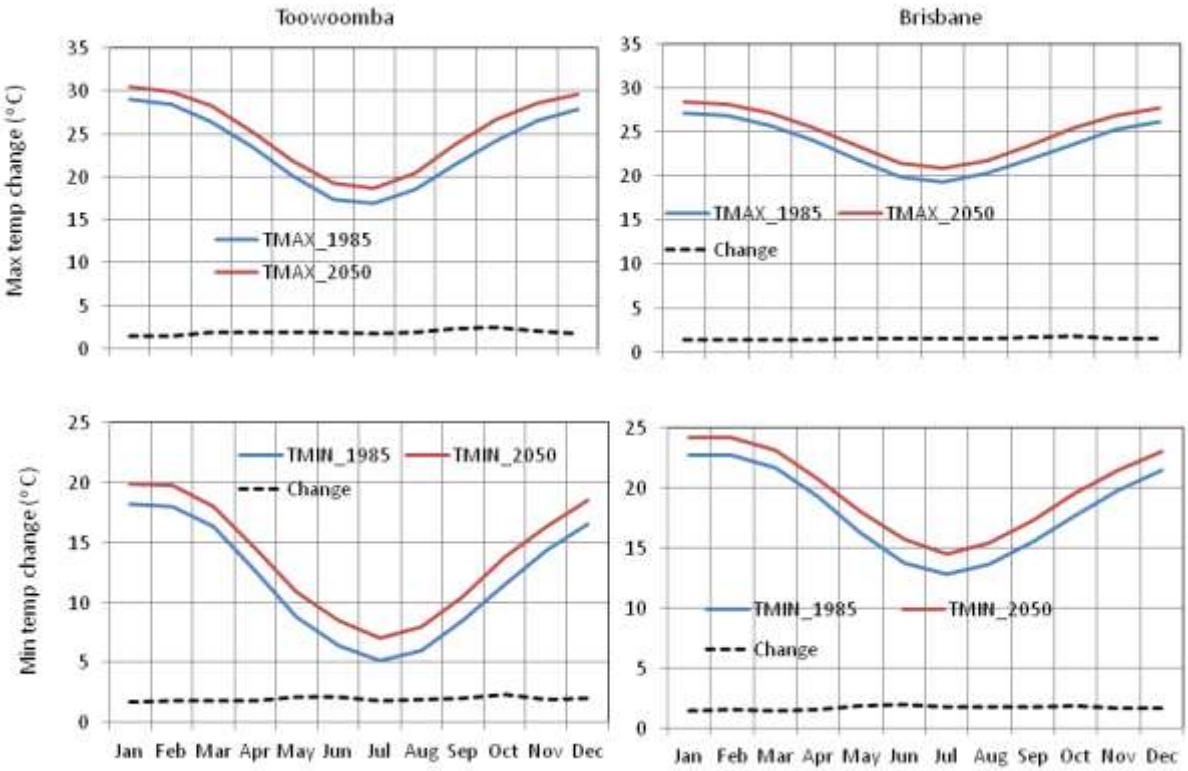

Figure 23: Change (oC) in maximum and minimum temperature at Toowoomba and Brisbane by 2050 relative to 1985.

2.3. Diurnal Temperature Range (DTR)

The diurnal temperature range (DTR) is calculated by subtracting daily minimum temperature from daily maximum temperature. Simulated DTR changes are shown in Figures 24 to 28.

In general, the NCAR CCSM3, INMCM3.0 and UKMO Hadgem1 models simulate an increase in the DTR for all seasons (except MAM in UKMO Hadgem1), which implies that, for these three CCAM downscaled runs, the rate of increase in the day time maximum temperature is faster than the rate of increase of night time minimum temperature. The other CCAM simulations show some increases and some decreases of DTR. For example MIROC Medres shows a small decrease in MAM and JJA (Figures 25 and 26), a large decrease in DJF (Figure 24) and small increases and decreases in SON (Figure 27). The ensemble-mean changes (Figure 28) show that DTR increases in SON and decreases in DJF, whereas MAM and JJA show some increases and some decreases.

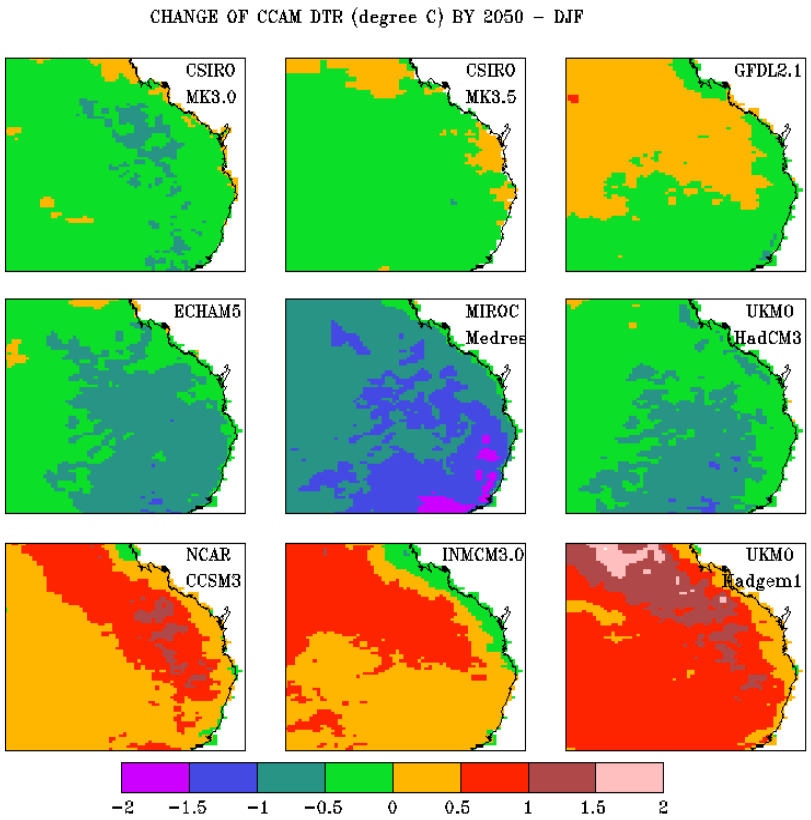

Figure 24: Change (°C) in diurnal temperature range for DJF by 2050 relative to 1985.

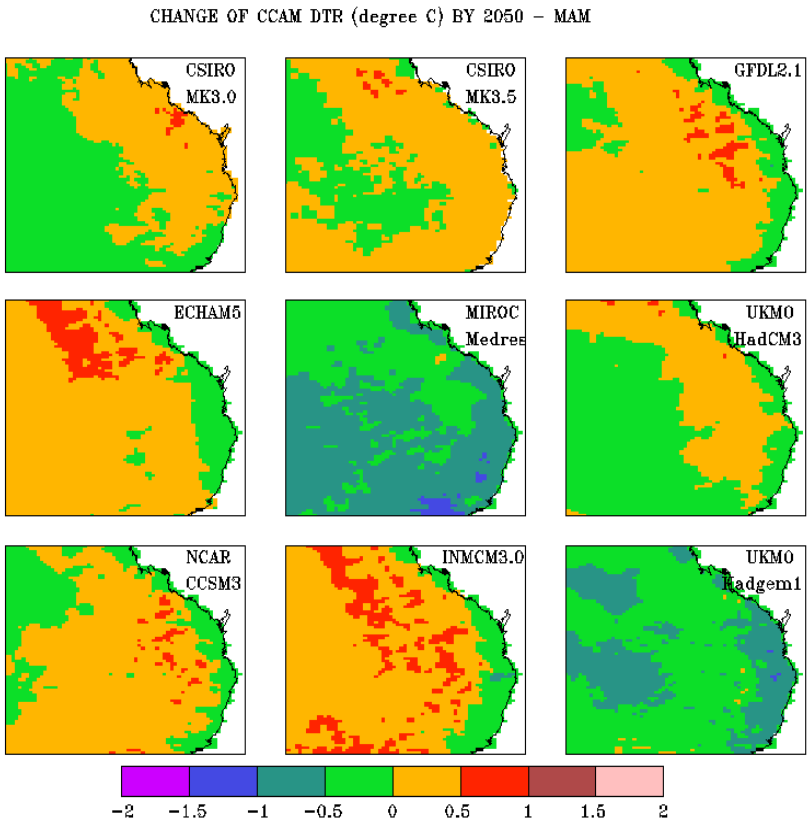

Figure 25: As in Figure 24 but for MAM.

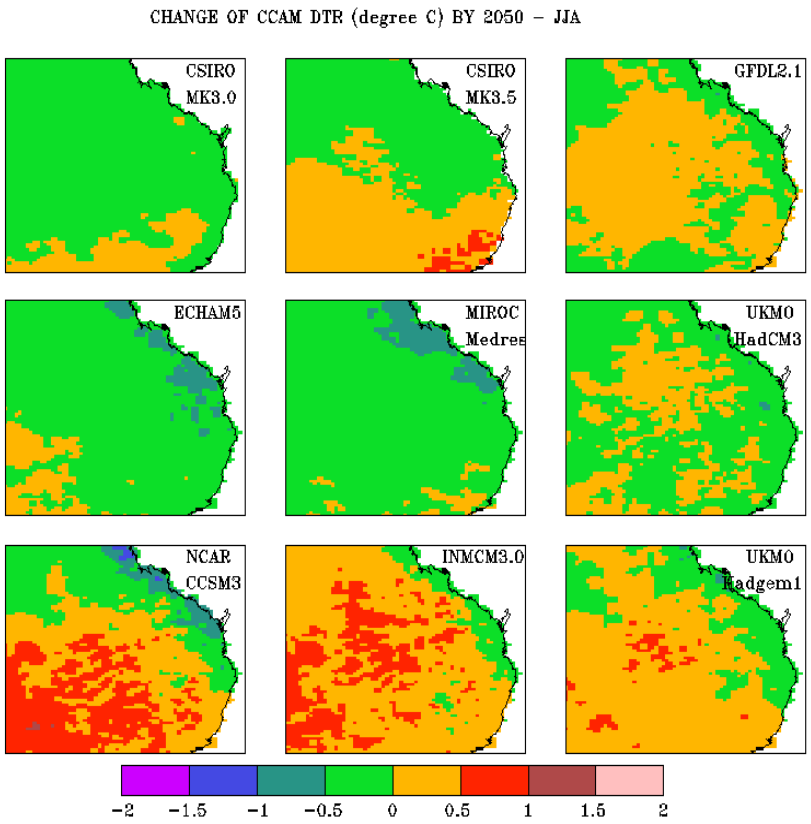

Figure 26: As in Figure 24 but for JJA.

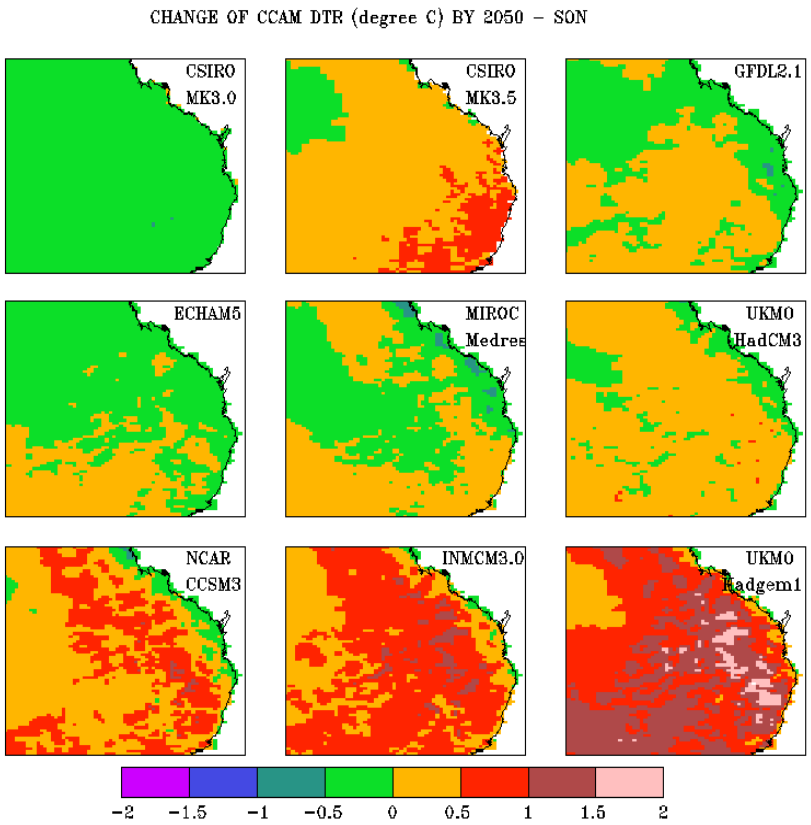

Figure 27: As in Figure 24 but for SON.

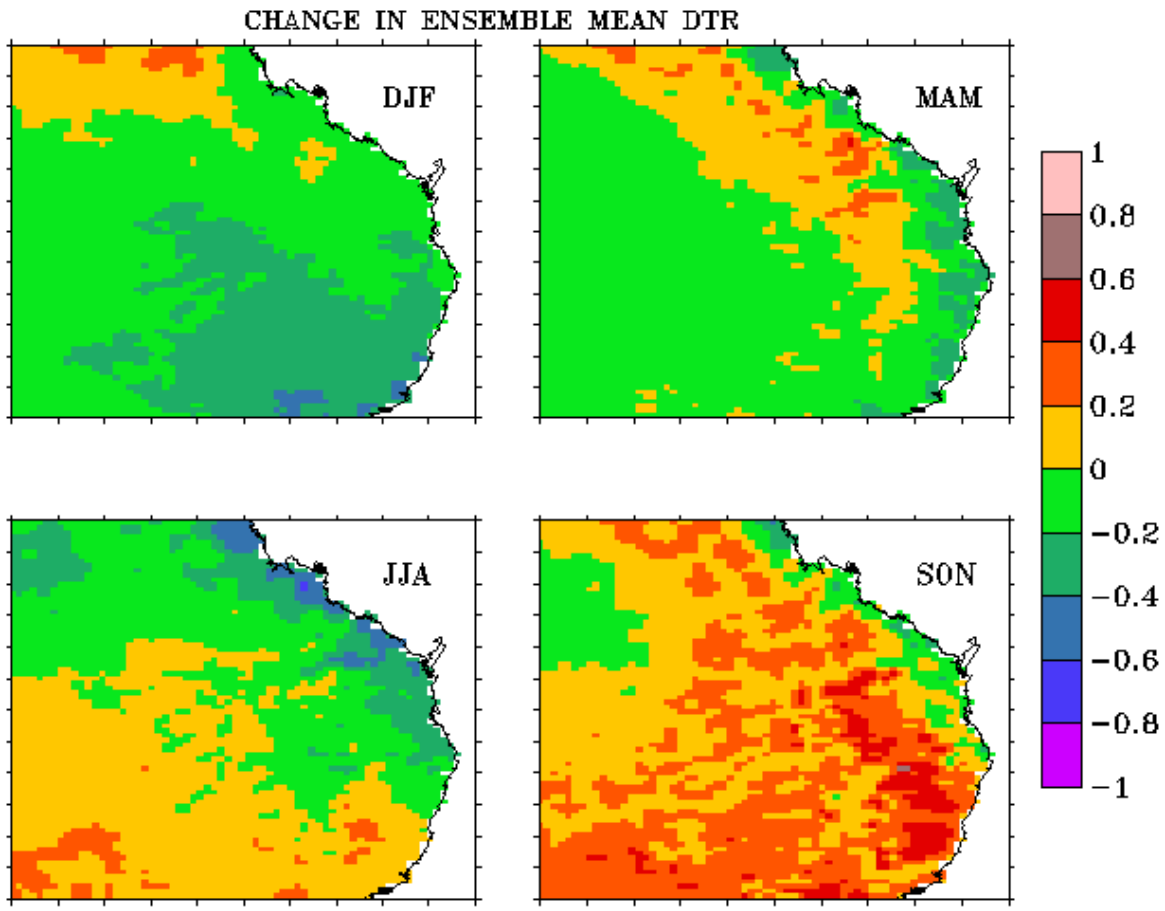

Figure 28: Seasonal change of the CCAM ensemble-mean DTR (oC) by 2050 relative to 1985.

2.4. Solar Radiation

Changes in solar radiation reaching the surface (Figures 29 to 33) are similar to the changes in maximum temperature discussed earlier. Across all seasons, the increase in solar radiation is largest (up to 10%) in NCAR CCSM3, INMCM3.0 and UKMO Hadgem1 (except MAM). The largest decrease is seen in DJF (Figure 29) with the MIROC Medres simulation showing reductions of around 10-20 W m^{-2} which correspond to decreases of 5-10% (not shown) when compared with the current climate. Note that the change in the relationship between maximum day time temperature and solar radiation is non-linear. For example, the largest maximum temperature decrease is in DJF for UKMO HadCM3, but its solar decrease is around 2%. Other factors that contribute to the changes in maximum and minimum temperatures are total cloud cover and relative humidity.

The percent decrease in the ensemble-mean solar radiation is around 2-3% (Figure 33). The solar radiation decreases in the south and increases in the north in DJF and MAM (Figure 33, upper left panel and upper right panel respectively). However, the pattern of change is reversed in JJA (winter season) compared to DJF (summer season), whereas in SON the solar radiation increases over most of the region.

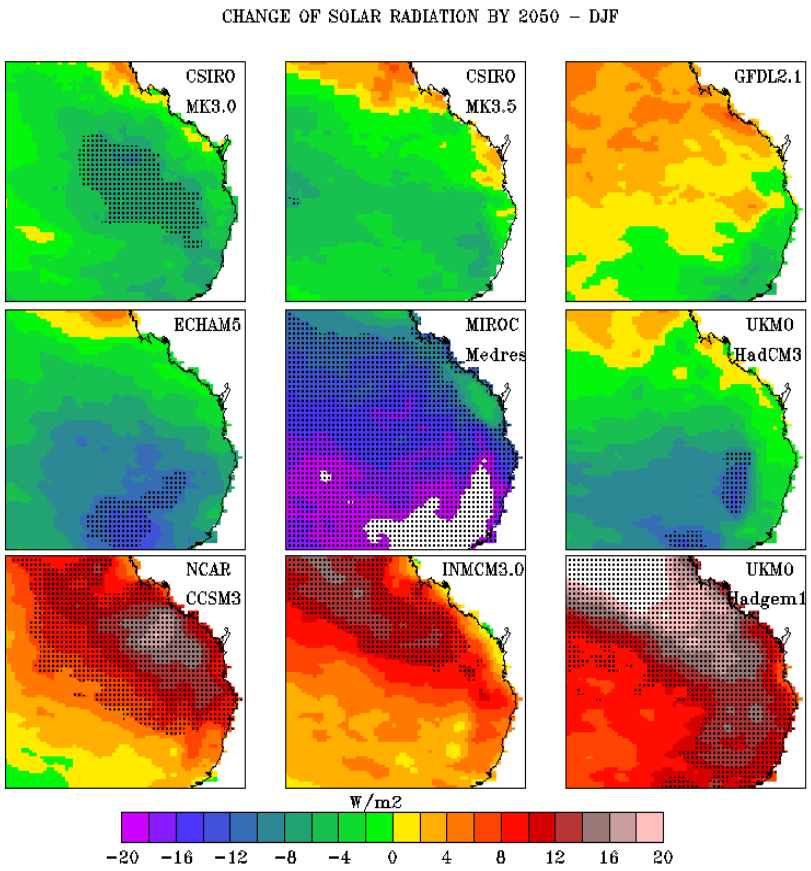

Figure 29: Change of solar radiation (W m-2) reaching the surface for DJF by 2050 relative to 1985.

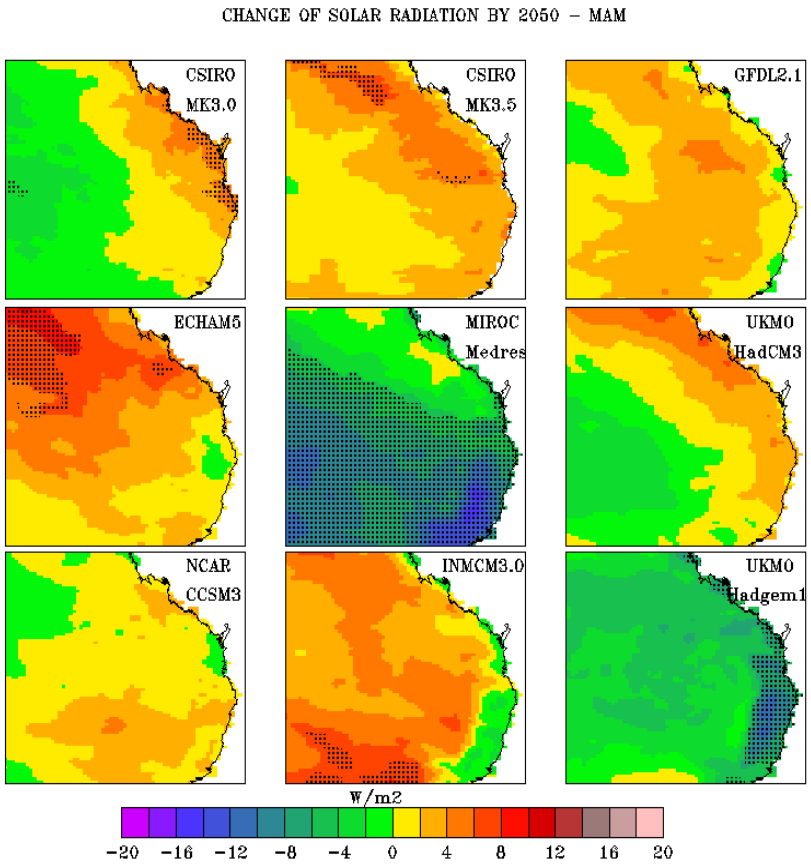

Figure 30: Change of solar radiation as in Figure 29 but for MAM.

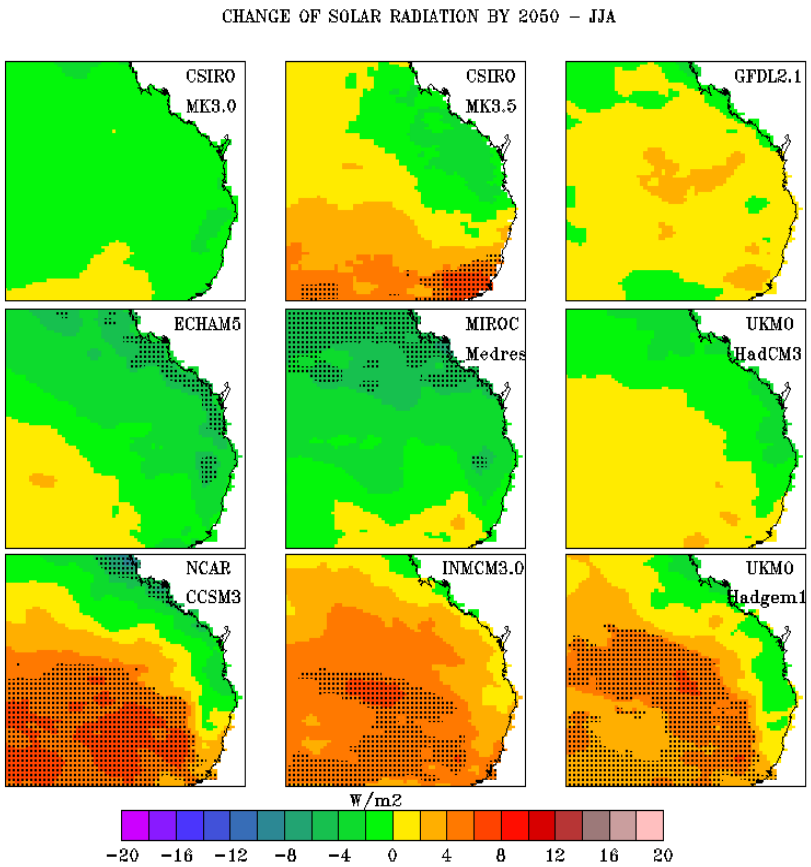

Figure 31: Change of solar radiation as in Figure 29 but for JJA.

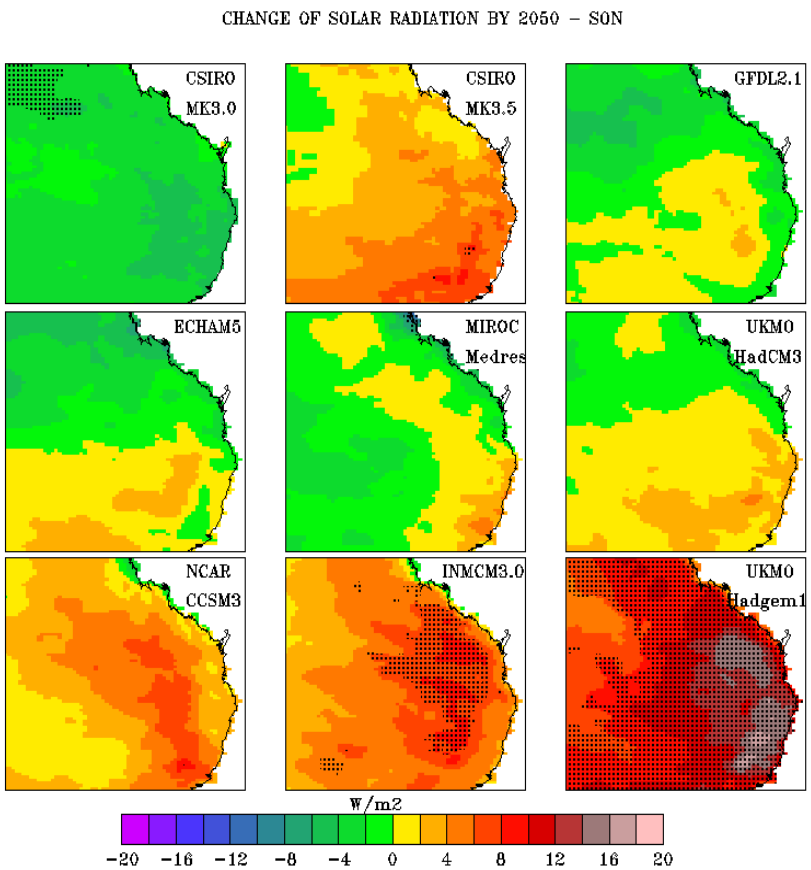

Figure 32: Change of solar radiation as in Figure 29 but for SON.

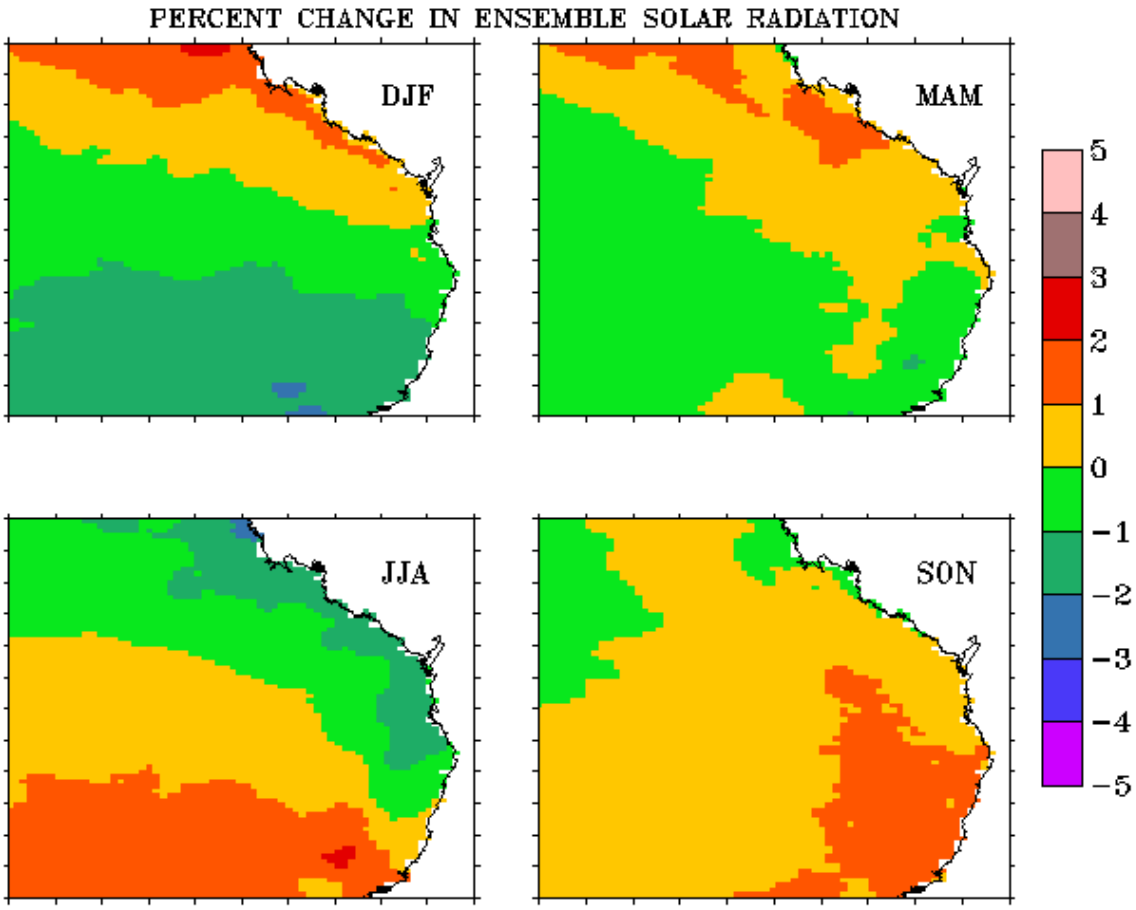

Figure 33: Percent change of CCAM ensemble-mean solar radiation (W m-2) reaching the surface by 2050 relative to 1985.

2.5. Relative Humidity

CCAM's projections of future change in the seasonal mean of relative humidity at 850 hPa are shown for the four seasons in Figures 34 to 38 for each CCAM ensemble member. The ensemble-mean change are shown at 850 hPa (Figures 38) and 200 hPa (Figures 39). The CCAM-simulated changes show both increases and decreases. In DJF (Figure 34), the largest increase in relative humidity at the low-level is projected by MIROC Medres. In contrast, the largest decrease is projected by UKMO-Hadgem1, INMCM3.0 and NCAR CCSM3; these reductions lie within the 95% confidence level. The largest reduction is projected for SON (Figure 37), where eight out of nine CCAM simulations agree (CSIRO MK3.0 gives a small but not significant increase). Relatively smaller changes are seen in MAM (Figure 35) and JJA (Figure 36).

At 850 hPa (Figure 38), the CCAM ensemble-mean is projected to increase slightly (less than 10%) in DJF and to slightly decrease in SON (also less than 10%). At 200 hPa (Figure 39), the changes are much stronger and increases of up to 35% are projected in the southern part of the domain in JJA and SON.

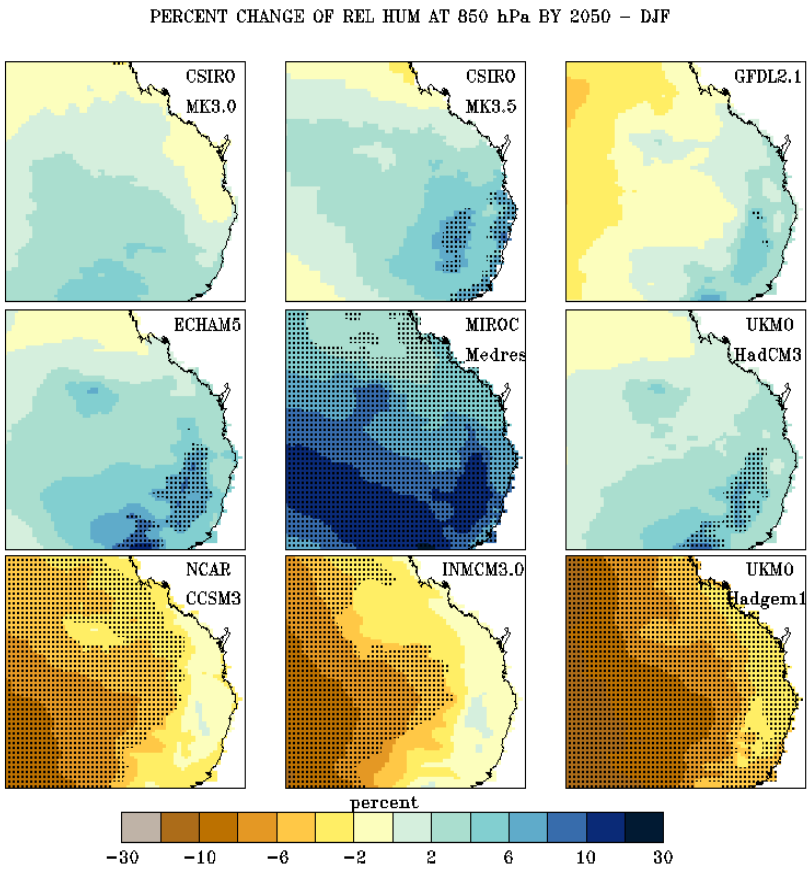

Figure 34: Change of relative humidity (%) at 850 hPa for DJF by 2050 relative to 1985.

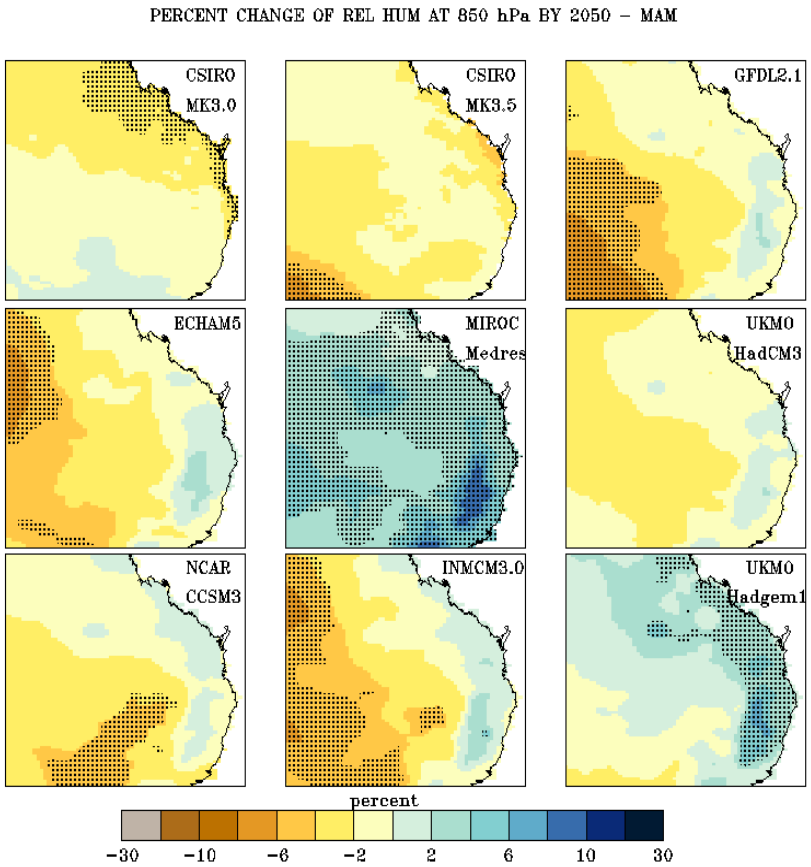

Figure 35: Change of relative humidity as in Figure 34 but for MAM.

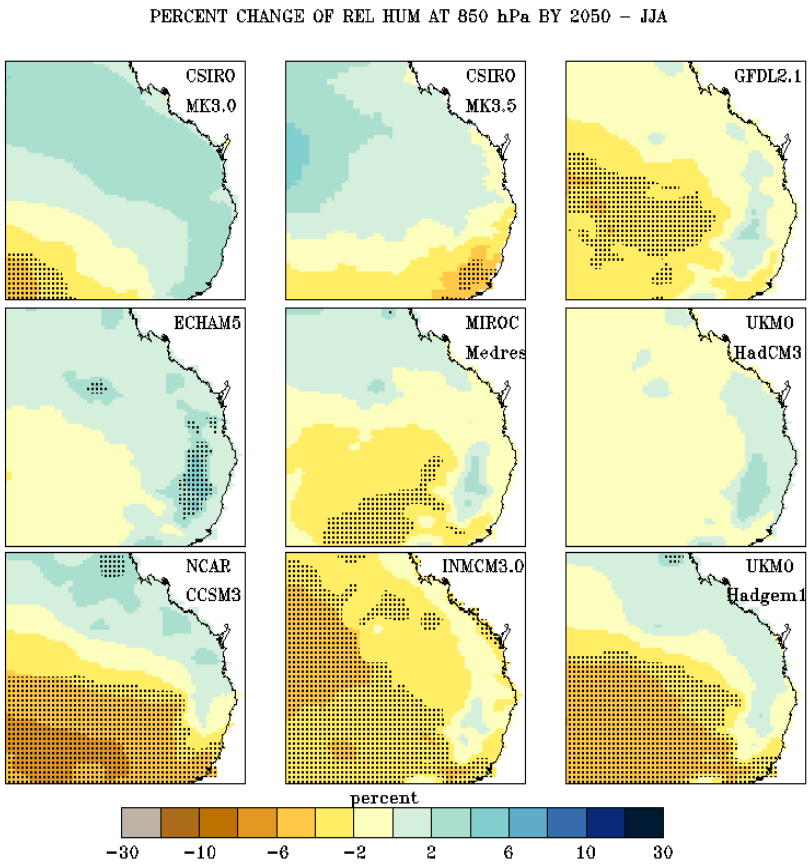

Figure 36: Change of relative humidity as in Figure 34 but for JJA.

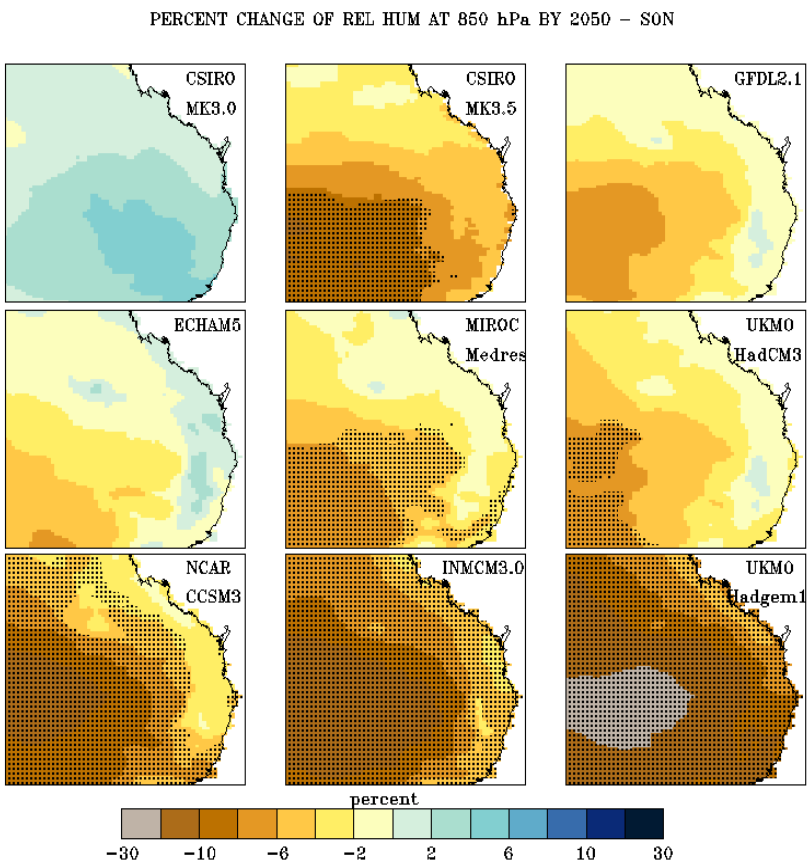

Figure 37: Change of relative humidity as in Figure 34 but for SON.

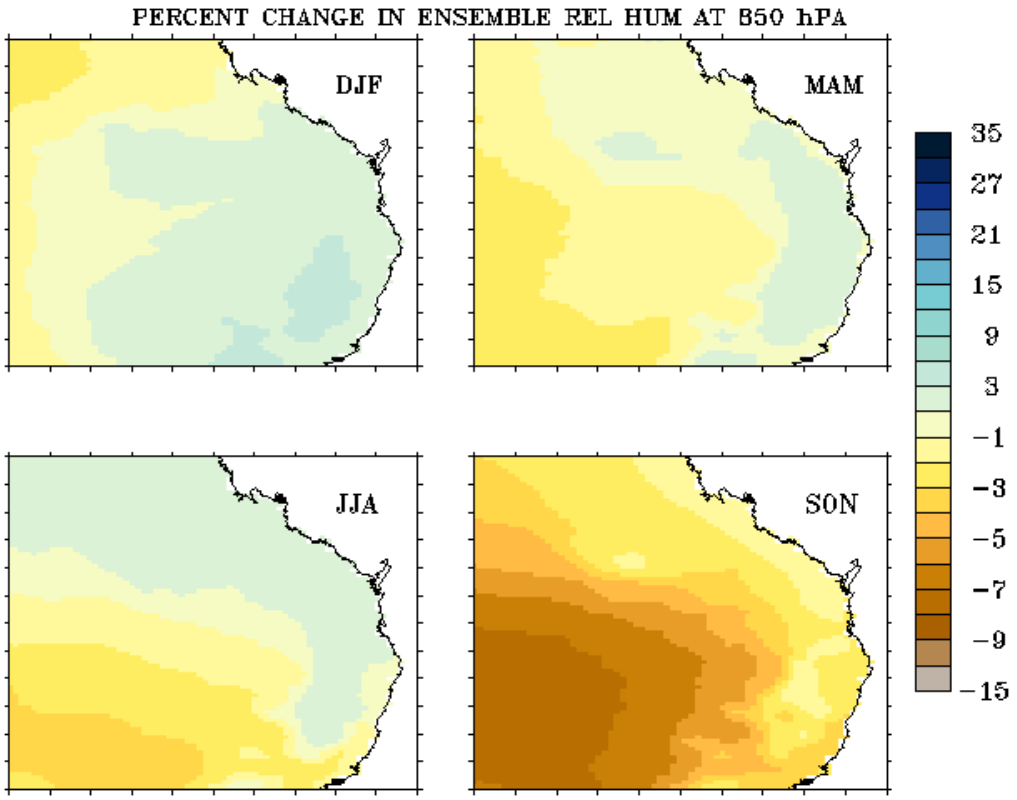

Figure 38: Change in relative humidity (%) at 850 hPa of the CCAM ensemble mean by 2050 relative to 1985.

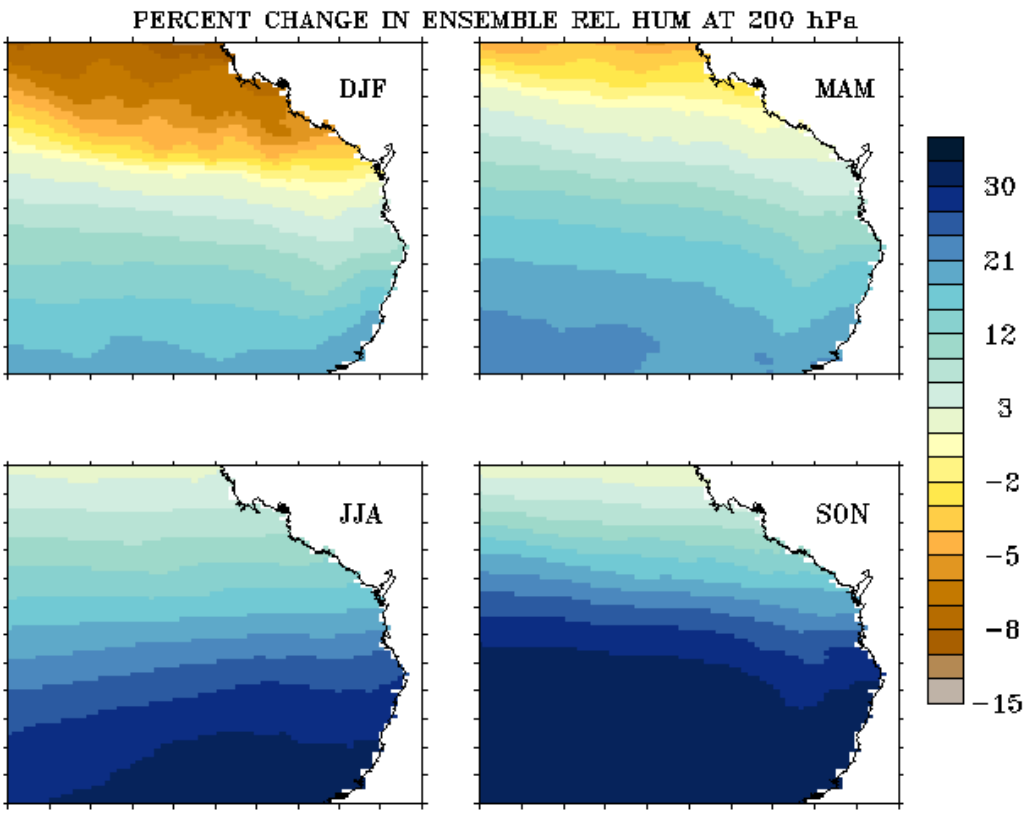

Figure 39: Change in relative humidity as in Figure 38 but at upper levels (200 hPa).

2.6. Wind Speed at 10 Metres

In general the simulated wind changes by 2050 are rather small (Figures 40 to 44), around 1 to 2 km/hour. In DJF (Figure 40) the wind speed is projected to be weaker, with statistical significance, by ECHAM5, MIROC Medres and UKMO HadCM3. The wind speed is predicted to increase by UKMO Hadgem1 but is statistically significant only for a small area. Whereas, other CCAM members predict increases in some parts of the domain and decreases in other parts of the domain but without statistical significance. In SON (Figure 43), wind speed increases are seen for all CCAM members, except for small decreases along the coast (Figure 43). The largest increase of around 8% is seen in UKMO Hadgem1 (Figure 43); in the other two seasons (JJA and MAM) the wind speed increases inland and decreases along the coast (Figures 41 and 42).

In term of percentage change (not shown) for DJF, MIROC Medres and ECHAM5 project the largest decreases of -10%, whilst UKMO HadCM3 projects the change to be about -6% to -8%. On the other hand, UKMO Hadgem1 projects the change to be around +2% to +6%. The largest percentage change, around +5% to +10%, is seen in MAM (Figure 41) from INMCM3.0 and UKMO Hadgem1. In JJA and SON, the percentage change is between +2% and +6%. The percentage change of the ensemble-mean wind at 10m is shown in Figure 44. In general, the change is between -5% (DJF) and +5% (SON). Also, the wind is weaker along the coast in DJF, MAM and JJA. The absolute change of the ensemble mean is small, between -0.5 and +0.5 km hour^{-1} (not shown) by 2050.

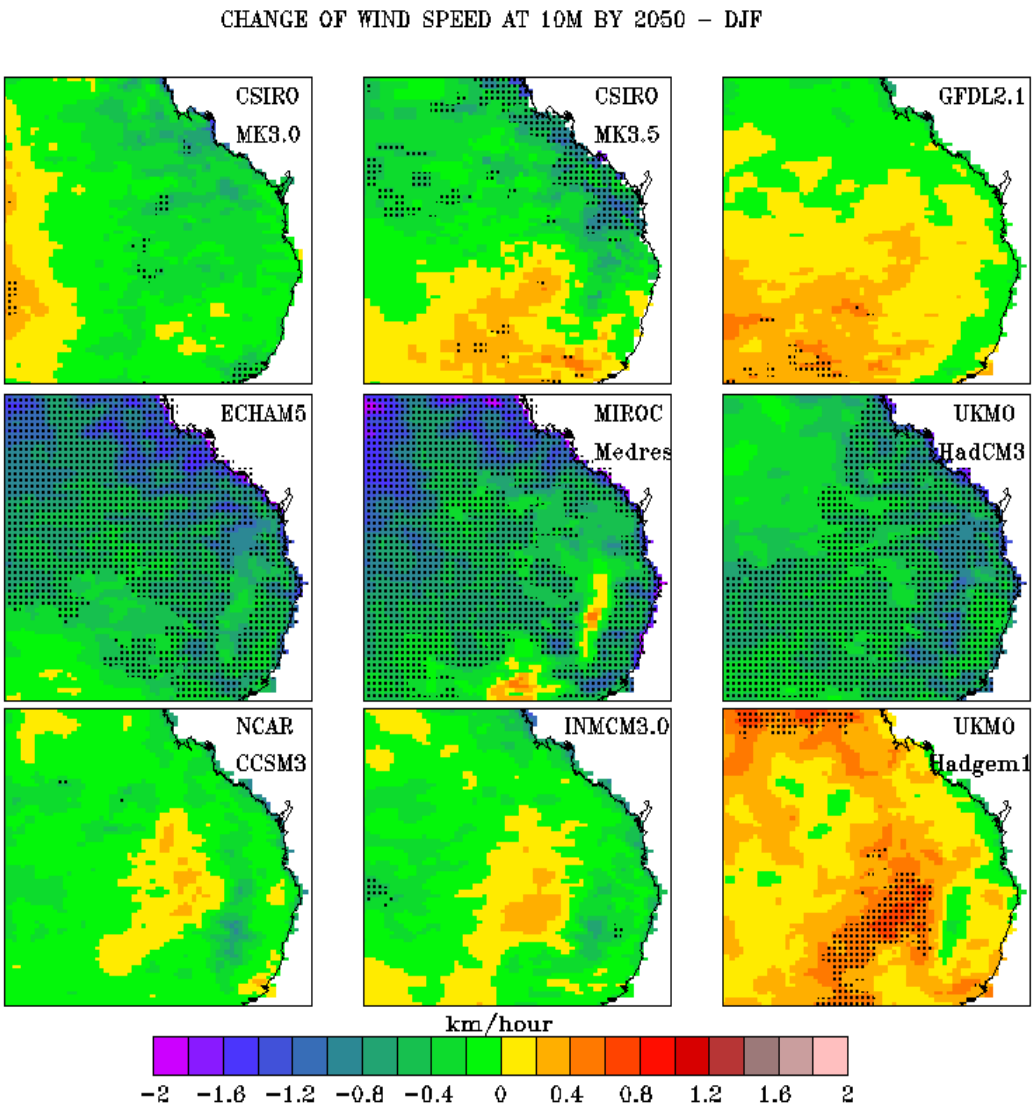

Figure 40: Change in wind speed (km hour-1) at 10 m for DJF by 2050 relative to 1985.

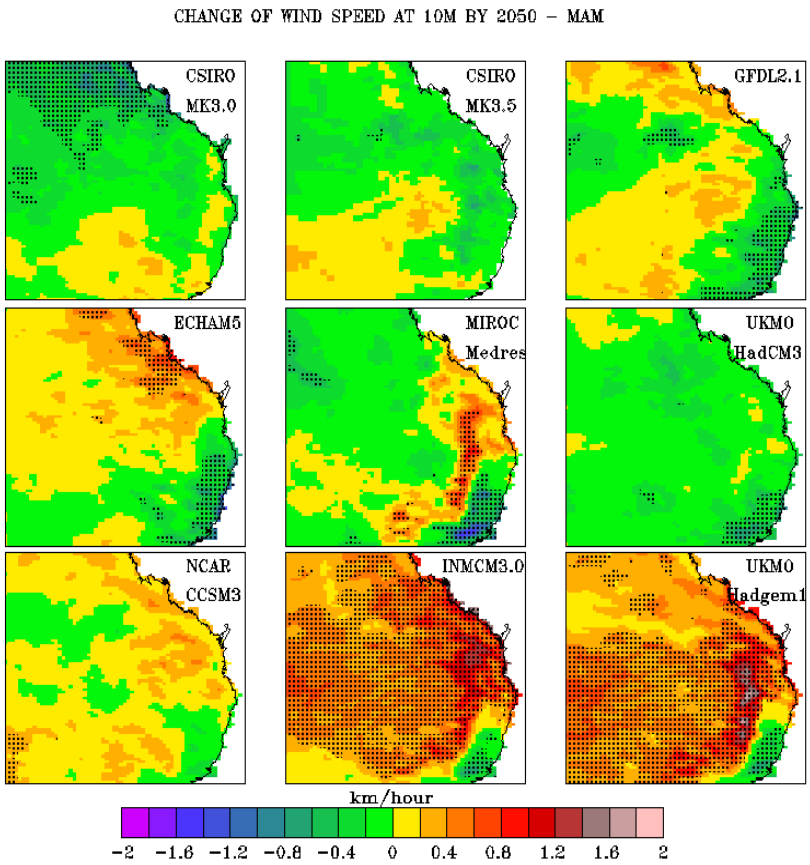

Figure 41: Change in wind speed as in Figure 40 but for MAM.

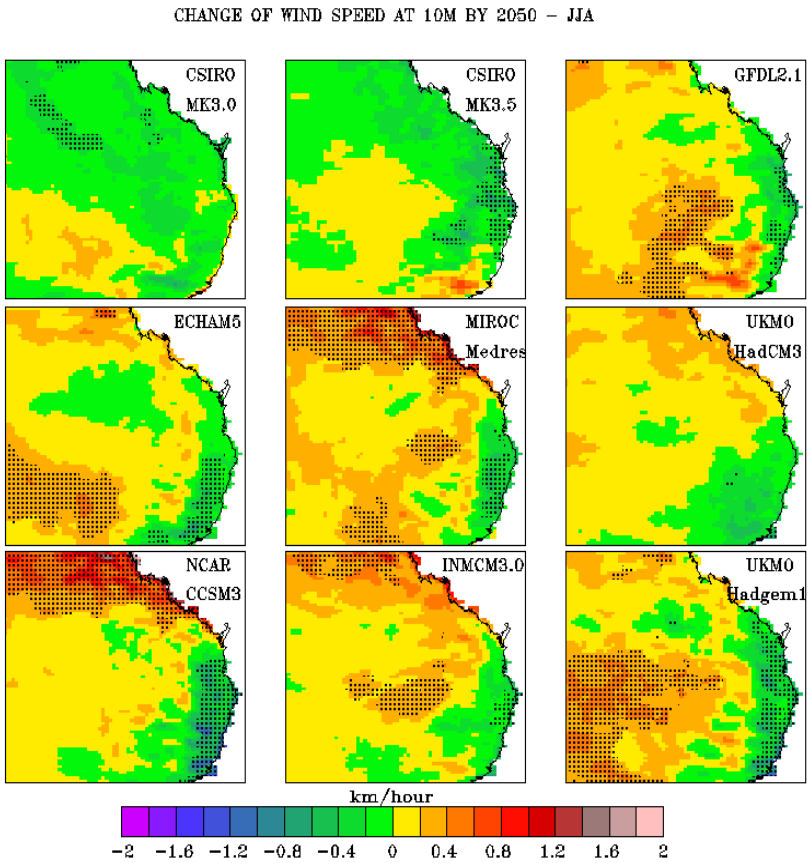

Figure 42: Change in wind speed as in Figure 40 but for JJA.

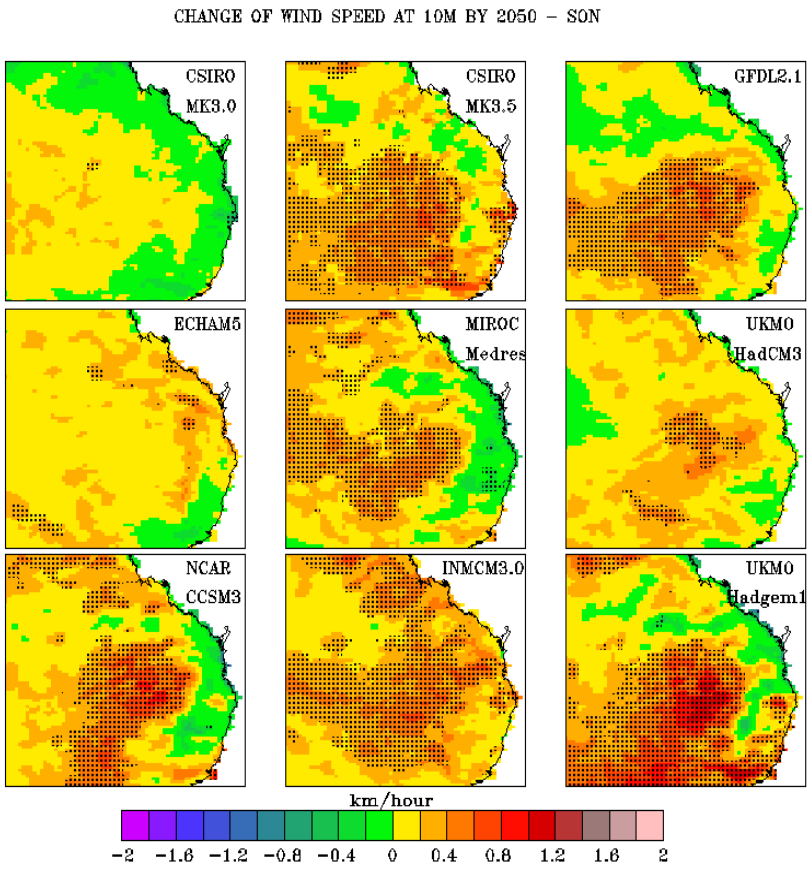

Figure 43: Change in wind speed as in Figure 40 but for SON.

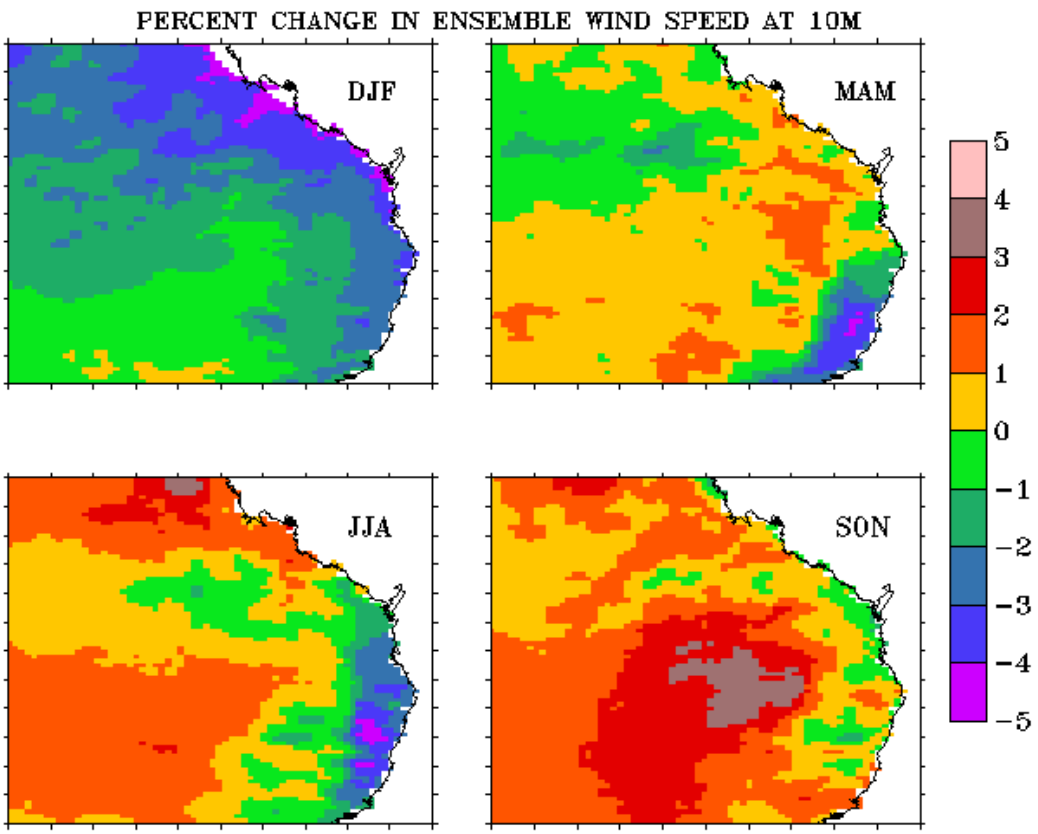

Figure 44: Change in wind speed as in Figure 40 but for percent change in CCAM ensemble mean.

2.7. Pan Evaporation

Projected changes in pan evaporation by CCAM are shown in Figures 45 to 49. According to the Student test, the change of this variable is significant at the 95% confidence level over the entire region. For clarity, stippling is not shown on the plot.

The pan evaporation is projected to generally increase by all simulation members. The strongest increases are in DJF (Figure 45), except for the northwest and southern domain in MIROC Medres and to some extent ECHAM5 and UKMO HadCM3. There are also strong increases in SON (Figure 48). The smallest increases are in JJA (Figure 47), whereas MAM (Figure 46) shows moderate increases. The largest percent increase (not shown) exceeds 35%, projected by UKMO Hadgem1 in SON.

The percentage change of the ensemble mean in Figure 49 shows that the pan evaporation is set to increase everywhere in the region and for all seasons. The largest increase is in SON (20%) and the smallest increase is in DJF (5-10%).

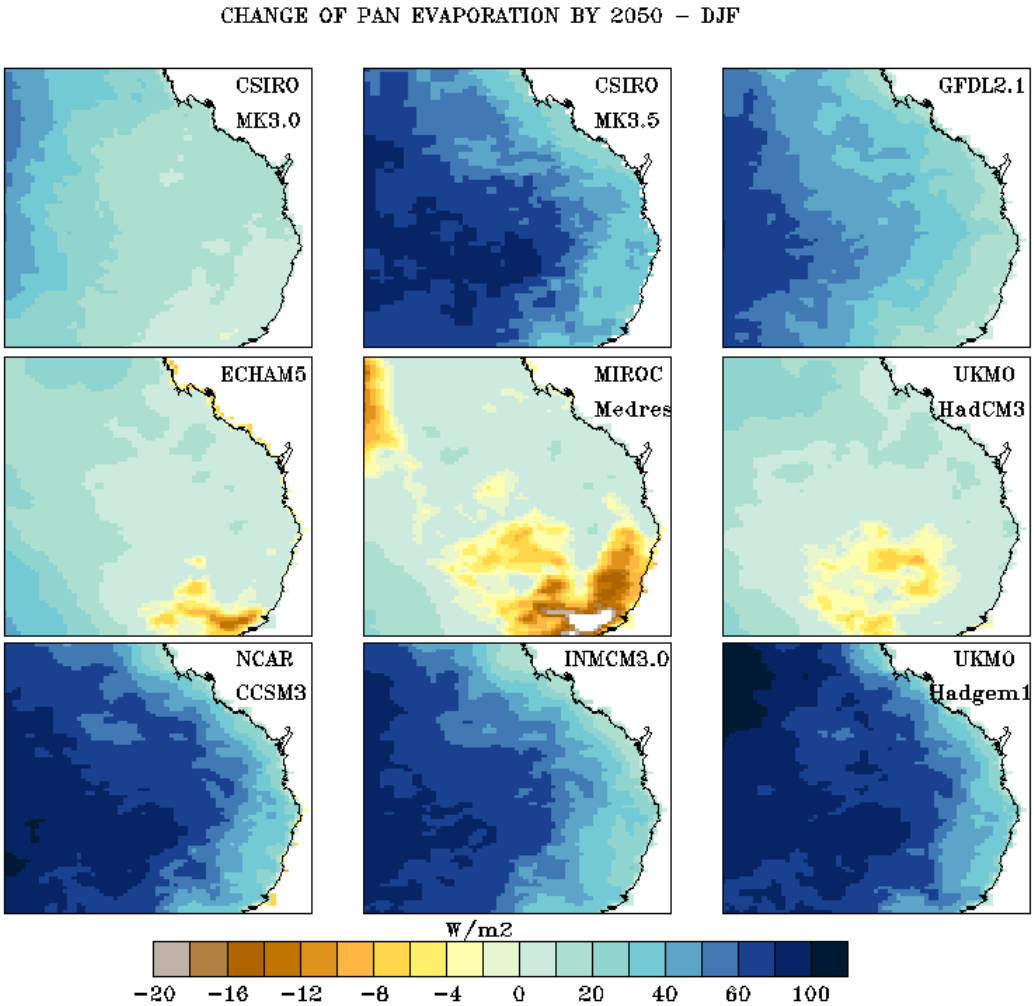

Figure 45: Change in pan evaporation (W m-2) for DJF by 2050 relative to 1985. Significance is at 95th level over most of the region, but not separately shown for clarity.

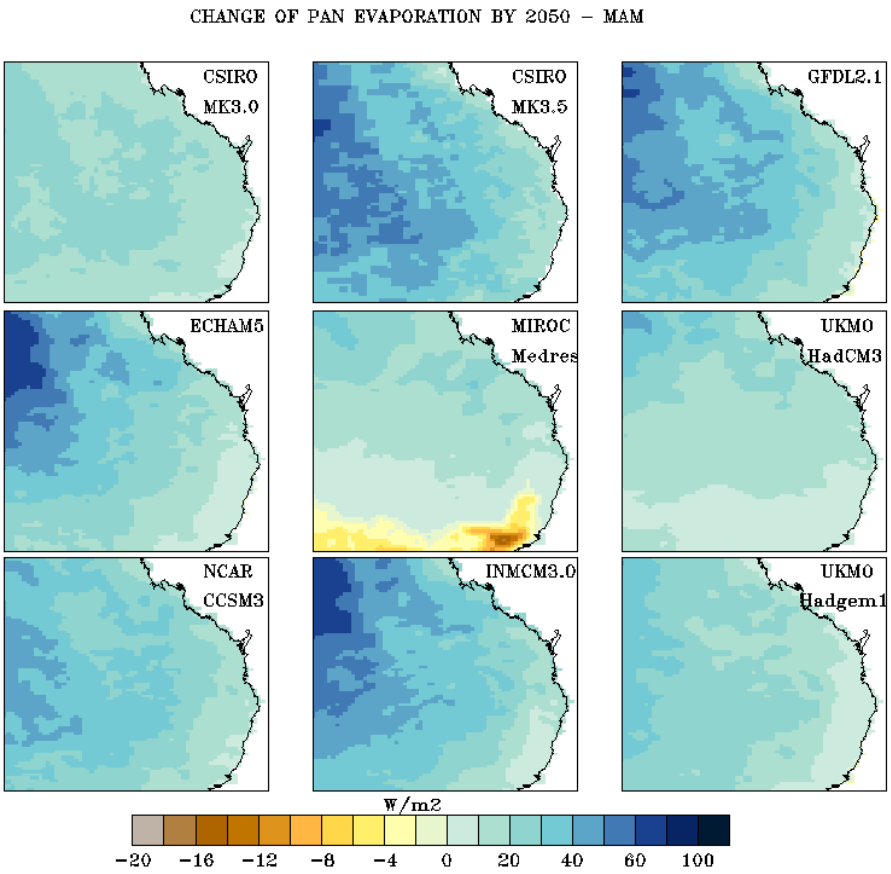

Figure 46: Change in pan evaporation as in Figure 45 but for MAM.

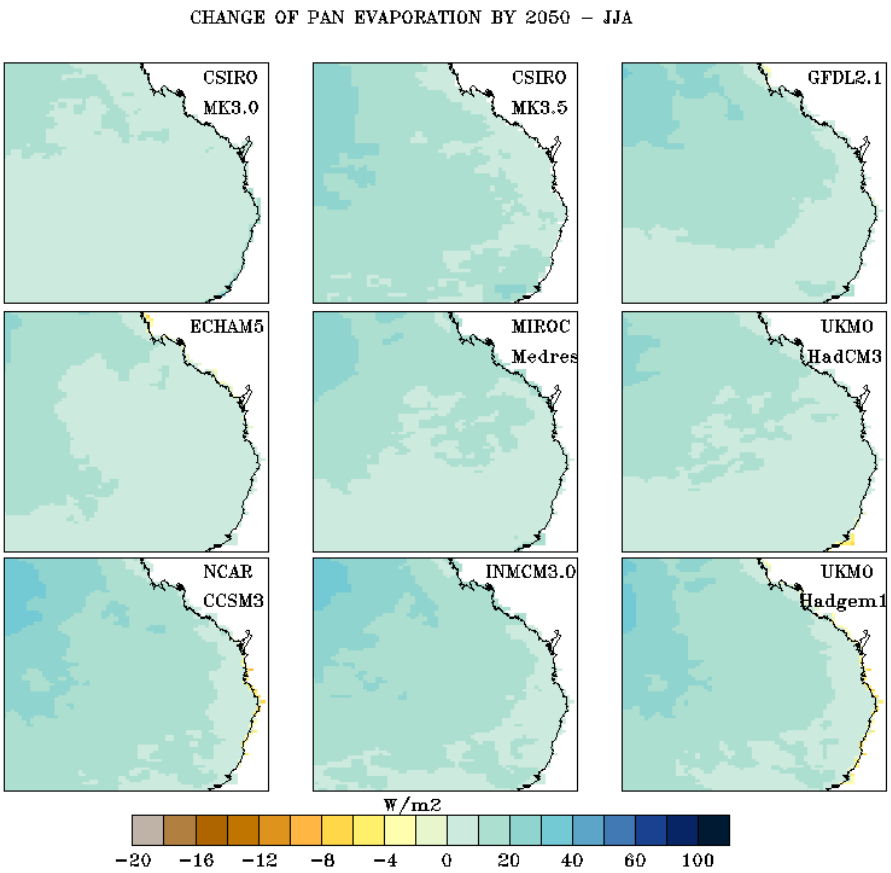

Figure 47: Change in pan evaporation as in Figure 45 but for JJA.

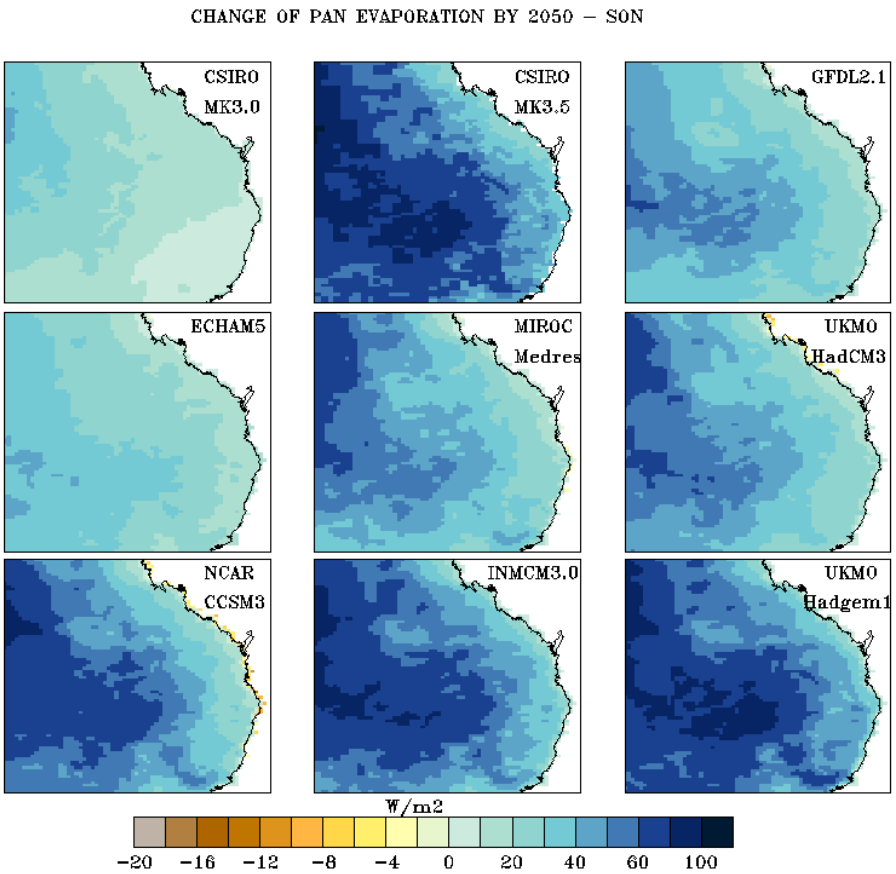

Figure 48: Change in pan evaporation as in Figure 45 but for SON.

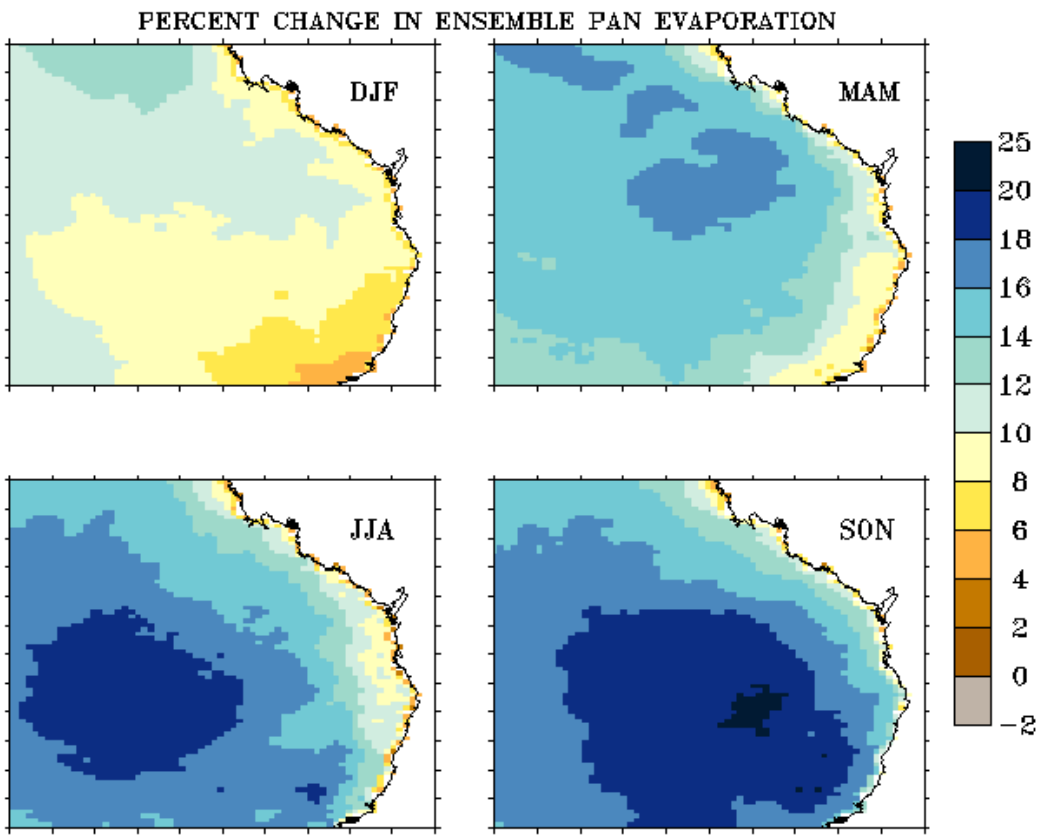

Figure 49: Percent change of ensemble-mean pan evaporation by 2050 relative to 1985.

3. SUMMARY

In summary, precipitation is the main driver of variability in the water balance (IPCC, Working Group II 2001). Hydrology and water resources are heavily link to precipitation. Small changes in precipitation may have serious consequences for both hydrology and water resources. By 2050, most CCAM ensemble members simulate a decrease from March to November for SEQ rainfall, with the strongest decreases of up to 15% near coastal regions in the transient seasons, MAM and SON. Summer rainfall is simulated to increase by up to 15% in the southern region, but only 10-20% of the CCAM members agree on this increase.

The maximum temperatures are simulated to increase in all seasons by 1.5-2.5^{o}C. Similar increases are seen for the minimum temperatures. In general, the solar radiation and the near- surface wind speeds are simulated to increase. The combination of increases in maximum temperature, solar radiation and wind speeds leads to increases in pan evaporation.

Except for DJF, the increases in evaporation without compensatory increases in precipitation are expected to lead to decreases in both soil moisture and runoff; in turn these could cause significant reductions in urban water supply and for irrigation of crops. It also has the potential to cause decreases in water quality related to changes in water tables and salinity. In addition, the warmer climate can be expected to lead to a greater incidence of tropical diseases in the southern regions, which will have potential impacts on people, livestock and native animals.

REFERENCES

IPCC (2001). Climate change 2001: Impacts, Adaptation, and Vulnerability. Contribution of Working Group II to the Third Assessment Report of the Intergovernmental Panel on Climate Change [Core Writing Team, McCarthy, J.J., Canziani O.F., Leary N.A., Dokken D.J. and White K.S. (eds)]. *IPCC*, Cambridge University Press.

McGregor, J.L., Gordon H.B., Watterson I.G., Dix M.R. and Rotstayn L.D. (1993). *The CSIRO 9-level atmospheric general circulation mode,* CSIRO Div. Atmospheric Research Tech. Paper No. 26, 89 pp.

McGregor, J.L. (2003). A new convection scheme using a simple closure, In *"Current issues in the parameterization of convection*", BMRC Research Report 93, 33-36.

McGregor J.L. (1996). Semi-Lagrangian advection on conformal-cubic grids, *Mon Weather Rev,* 124: 1311-1322.

McGregor J.L. (2005a). Geostrophic adjustment for reversibly staggered grids, *Mon Weather Rev,* 133: 1119-1128.

McGregor J.L. (2005b). C-CAM: Geometric aspects and dynamical formulation [electronic publication], *CSIRO Atmospheric Research Technical Paper 70*, 43 pp.

McGregor, J.L. and Dix M.R. (2008). An updated description of the Conformal-Cubic Atmospheric Model, In *High Resolution Simulation of the Atmosphere and Ocean*, eds. K. Hamilton and W. Ohfuchi, Springer, 51-76.

Nguyen K.C., Katzfey J.J. and McGregor J.L. (2011). Global 60 km simulation with CCAM: Evaluation over the tropics, *Climatic Dynamics*, doi: 10.1007/s00382-011-1197-8.

Nguyen K.C. and McGregor J.L. (2012). *Numerical simulation of current climate conditions for South East Queensland.* Urban Water Security Research Alliance Technical Report No. 78.

Thatcher, M. and McGregor J.L. (2008). Using a scale-selective filter for dynamical downscaling with the conformal cubic atmospheric model, *Mon. Wea. Rev*., 137, 1742-1752.

Urban Water Security Research Alliance